FLUX MEASUREMENTS OF VOLATILE ORGANIC COMPOUNDS FROM AN URBAN TOWER PLATFORM

A Dissertation

by

CHANG HYOUN PARK

Submitted to the Office of Graduate Studies of
Texas A&M University
in partial fulfillment of the requirements for the degree of

DOCTOR OF PHILOSOPHY

May 2010

Major Subject: Atmospheric Sciences

FLUX MEASUREMENTS OF VOLATILE ORGANIC COMPOUNDS FROM AN URBAN TOWER PLATFORM

A Dissertation

by

CHANG HYOUN PARK

Submitted to the Office of Graduate Studies of
Texas A&M University
in partial fulfillment of the requirements for the degree of

DOCTOR OF PHILOSOPHY

Approved by:

Chair of Committee,	Gunnar W. Schade
Committee Members,	Renyi Zhang
	Don Collins
	Shari Yvon-Lewis
Head of Department,	Kenneth Bowman

May 2010

Major Subject: Atmospheric Sciences

ABSTRACT

Flux Measurements of Volatile Organic Compounds from an Urban Tower Platform.

(May 2010)

Chang Hyoun Park, B.S., Pusan National University;

M.S., Pusan National University

Chair of Advisory Committee: Dr. Gunnar W. Schade

A tall tower flux measurement setup was established in metropolitan Houston, Texas, to measure trace gas fluxes from both anthropogenic and biogenic emission sources in the urban surface layer. We describe a new relaxed eddy accumulation system combined with a dual-channel gas chromatography - flame ionization detection used for volatile organic compound (VOC) flux measurements in the urban area, focusing on the results of selected anthropogenic VOCs, including benzene, toluene, ethylbenzene and xylenes (BTEX), and biogenic VOCs including isoprene and its oxidation products, methacrolein (MACR) and methyl vinyl ketone (MVK). We present diurnal variations of concentrations and fluxes of BTEX, and isoprene and its oxidation products during summer time (May 22 – July 22, 2008) and winter time (January 1 – February 28). The measured BTEX values exhibited diurnal cycles with a morning peak during weekdays related to rush-hour traffic and additional workday daytime flux maxima for toluene and xylenes in summer time. However, in winter time there was no additional workday daytime peaks due mainly to the different flux footprints between the two seasons. A

comparison with different EPA National Emission Inventories (NEI) with our summer time flux data suggests potential underestimates in the NEI by a factor of 3 to 5.

The mixing ratios and fluxes of isoprene, MACR and MVK were measured during the same time period in summer 2008. The presented results show that the isoprene was affected by both tail-pipe emission sources during the morning rush hours and biogenic emission sources in daytime. The observed daytime mixing ratios of isoprene were much lower than over forested areas, caused by a comparatively low density of isoprene emitters in the tower's footprint area. The average daytime isoprene flux agreed well with emission rates predicted by a temperature and light only emission model (Guenther et al., 1993). Our investigation of isoprene's oxidation products MACR and MVK showed that both anthropogenic and biogenic emission sources exist for MACR, while MVK was strongly dominated by a biogenic source, likely the isoprene oxidation between the emission and sampling points.

DEDICATION

To my dear father, mother, brother and aunt.

ACKNOWLEDGEMENTS

I am heartily thankful to my advisor, Dr. Gunnar W. Schade, who has been guiding and supporting me from the initial to the final level in an understanding of this subject. I've learned many things from him, especially how to think with reasoned thoroughness on scientific themes, and a passion for a science. I appreciate his always being patient with me.

I am thankful to my committee members: Dr. Renyi Zhang, who taught me in my first year of course work when I had no idea of atmospheric chemistry, and always has smiled and asked me about the progress of my research whenever we've met in an elevator or walked together; Dr. Don Collins, who motivated me to choose this school for my Ph.D. study in the first stages of my application, and partially supported me financially in my first year; and Dr. Shari Yvon-Lewis, who was willing to be on my committee, and guided and encouraged me through my research when I felt this study was a huge unconquestable mountain as well as a never-ending story.

I am also thankful to all my teachers: Dr. Kenneth Bowman, who was willing to be my advisor temporarily in my first year; Dr. Craig Epifanio and Dr. Ping Yang, who also gave me the opportunity to be a grader for their dynamics, and physics classes, respectively; Dr. Fuqing Zhang (now at Penn State University); Dr. Courtney Schumacher; Dr. Sarah D. Brooks; and Dr. Gerald R. North.

I offer my regards and blessings to all of those who have been working and studying with me in the Department of Atmospheric Sciences at Texas A&M University, especially to Naruki Hiranuma (Seong-Gi Moon), Lijun Zhou and Ian Boedeker, who have spent many years with me as office mates, and Kaycee Bevers and her husband, Matt Bevers, who showed me sincerity.

I also offer my blessings to the alumni of Pusan National University at Texas A&M, and all members of the A&M Korean Student Church and the Vision Mission Church in College Station, Texas.

Lastly, I thank God, who is the first cause of the existence of all creatures in the world from the big bang to this moment, and most of all gave me the meaning of life.

TABLE OF CONTENTS

Page

LIST OF FIGURES

Page

LIST OF TABLES

Page

1. INTRODUCTION

Air quality studies overwhelmingly focus on the concentration of US Environmental Protection Agency (EPA) criteria air pollutants using monitoring and numerical modeling. While the latter uses surface fluxes from emission inventories as input, the true emission rate based on "top-down" measurements of flux – instead of concentration only – has rarely been established. However, the pollutant flux, i.e. how much mass moves through a unit area per unit time, is required to validate the emission inventory, to understand real atmospheric pollutant dynamics, and ultimately to evaluate the current photochemical modeling schemes.

Flux measurements of volatile organic compounds (VOCs) emitted from forests are now routinely carried out with various micrometeorological techniques, including eddy covariance, disjunct eddy covariance and relaxed eddy accumulation (REA) (Ciccioli et al., 2003; Gallagher et al., 2000; Grabmer et al., 2004; Karl et al., 2001; Karl et al., 2002; Olofsson et al., 2003; Rinne et al., 2001; Rinne et al., 2008; Valentini et al., 1997; Warneke et al., 2002). However, few flux measurements have targeted urban areas yet (Karl et al., 2009; Langford et al., 2009; Langford et al., 2010; Velasco et al., 2005a; Velasco et al., 2009), presumably due to the physically complicated urban environment, a complex mix of anthropogenic and biogenic emission sources, and a lack of suitable or economically accessible measurement locations. Yet, this lack of urban flux

---

This dissertation follows the style of Agricultural and Forest Meteorology.

measurements occurs despite urban air pollution's significant direct and indirect effects on atmospheric chemistry and public health.

Urban air pollution sources are related to a multitude of land-uses and human-made structures, which, together with natural and introduced vegetation, make up the urban fabric. To measure pollutant flux over urban terrain, a tall platform must be found that does not influence the wind itself while allowing a measurement setup. The system should be located at minimally twice the urban canopy height and ideally higher to avoid the urban roughness layer (Roth, 2000) and observe an integrated effect from what is called an upwind footprint area. Previous such studies have been limited to a few cities: Nemitz et al. (2002) and Dorsey et al. (2002) measured particle and CO_2 fluxes above the city of Edinburgh, UK, while Mårtensson et al. (2006) measured aerosol fluxes in Stockholm. Grimmond et al. (2002) reviewed urban CO_2 measurements and reported their own measurements of CO_2 mixing ratios and fluxes for Chicago, USA. Soegaard and Möller-Jensen (2003) reported measurements of CO_2 fluxes over the city of Copenhagen. Both CO_2 and VOC flux measurements were carried out in Mexico City in 2003 by Velasco et al.(Velasco et al., 2005a; Velasco et al., 2005b). More recently, detailed urban VOC flux measurements have been reported by Langford and coworkers for urban Manchester (Langford et al., 2009) and London (Langford et al., 2010).

In Houston, Texas, the US's 4th largest metropolitan area, located in a subtropical climate, air quality with respect to ozone and particulate matter remains poor. Ground-

level ozone concentrations in violation of the National Ambient Air Quality Standard (NAAQS) occur regularly between April and October (Banta et al., 2005). Owing to the largest number of petrochemical facilities in the nation, ozone in exceedance of the NAAQS is commonly caused by higher ozone production rates than found in most other major cities in the United States (Daum et al., 2003; Daum et al., 2004). It is often the result of regionally high VOC emissions in its industrial ship channel, adding to already high amounts of car traffic emissions (Berkowitz et al., 2005; Gilman et al., 2009; Jiang and Fast, 2004; McGaughey et al., 2004; Qiao et al., 2005). The EPA forecasts that Harris County, to which Houston belongs, is likely to still violate the new 8-h NAAQS of 75 ppb in 2020 (Strengthened National Standards for Ground-Level Ozone, http://www.epa.gov/air/ozonepollution/actions.html), which is indicated in the Figure 1.1.

Benzene, toluene, ethylbenzene and xylenes (BTEX) are the most abundant aromatic components of VOCs in the atmosphere in urban areas. They stem mainly from vehicle exhaust, gasoline evaporation and other emissions from solvent/paint uses and natural gas leaks (Song et al., 2007). BTEX species can also play an important role in the atmospheric chemistry as the precursors for tropospheric ozone (Atkinson, 1990) and secondary organic aerosols (Dechapanya et al., 2003; Henze et al., 2008; Kelly et al., 2010; Myriokefalitakis et al., 2008; Na et al., 2003; Rappengluck et al., 1999; Vlasenko et al., 2009).

Figure 1.1. Map of counties with monitors projected to violate the 2008 8-hour ozone standard of 75ppb in 2020. (http://www.epa.gov/air/ozonepollution/pdfs/2008_03_monitors_projected_violate_2020.pdf)

The evaluation of the oxidation of BTEX compounds is useful, for example as indicators of chemical aging using the ratios of benzene/toluene (B/T) and ethylbenzene/m,p-xylene (E/X) (Nelson and Quigley, 1983; Roberts et al., 1984). Negative effects on public health are also of concern: long-term exposure to BTEX can cause peripheral neuropathy and toxic encephalopathy, such as memory loss and impaired cognition (Baker et al., 1985), and auditory neuropathy (Draper and Bamiou, 2009). In addition, benzene is known as a human carcinogen (Mehlman, 1990; Whitworth et al., 2008). Numerous field and modeling studies have been carried out in Houston with a focus on its Ship Channel, due to the fact that its petrochemical industries are known as large point sources for VOCs, including BTEX, affecting local air quality (Banta et al., 2005; Berkowitz et al., 2005; Carslaw et al., 2007; Gilman et al., 2009; Hanna et al., 2007;

Karl et al., 2003; McGaughey et al., 2004; Na et al., 2003; Qiao et al., 2005; Raun et al., 2009; Reiss, 2006; Smith et al., 2007).

Among the VOCs that play an important role in the formation of ozone and secondary organic aerosols, isoprene represents the single highest emissions into the troposphere (Guenther et al., 2006). Once in the lower atmosphere isoprene is oxidized mainly by OH radicals during daytime, and O_3 and NO_3 radicals during nighttime. Its major oxidation products as a result of the OH-initiated oxidation in a NOx-rich environment are formaldehyde, methacrolein (MACR), and methyl vinyl ketone (MVK) (e.g (Carter and Atkinson, 1996; Tuazon and Atkinson, 1990)), which account for approximately 50-60% of the carbon yield. Isoprene's emission sources are overwhelmingly dominated by higher plants which possess the enzyme isoprene synthase (Kuzma and Fall, 1993; Monson et al., 1992).

Due to its importance in atmospheric chemistry, numerous field campaigns have investigated isoprene's chemistry in-situ, often through measurements of its principal oxidation products MACR and MVK both at rural and forest sites (Apel et al., 2002; Dreyfus et al., 2002; Helmig et al., 1998; Montzka et al., 1995; Montzka et al., 1993; Roberts et al., 2006; Spaulding et al., 2003; Starn et al., 1998; Stroud et al., 2001; Warneke et al., 2001; Wiedinmyer et al., 2001), and more polluted urban or near-urban sites (Geron et al., 1995; Karl et al., 2002; Kleinman et al., 2005; Riemer et al., 2008; Stroud et al., 2001). While the goals of these studies varied, their findings were largely

in good agreement with results from controlled laboratory studies, such as the carbon yield from isoprene or the development of the MACR to MVK ratio. It was found that due to its high reactivity, isoprene can contribute dominantly to regional ozone formation given significant anthropogenic NOx emissions (Dreyfus et al., 2002).

The emission of isoprene from emitting plant species is influenced strongly by incident radiation and leaf temperature. Typical emitters are found among the Fagaceae family, such as many oak tree species (Singsaas and Sharkey, 1998; Singsaas and Sharkey, 2000; Tambunan et al., 2006). The most common algorithm used to describe plant isoprene emissions consists of essentially three terms, a so-called 'basal isoprene emission rate', which is generally obtained from controlled leaf-level emission experiments (Fall and Wildermuth, 1998; Guenther et al., 1991; Guenther et al., 1993), and temperature and light correction terms, as follows:

$$I = I_s \cdot C_T \cdot C_L \qquad (1.1)$$

where I is the instantaneous isoprene emission rate, I_S the isoprene basal emission rate, C_T the temperature correction term, and C_L the light correction term. The influence of temperature and light on isoprene's emission rate, the factors C_T and C_L, were originally based on leaf enzyme kinetics (Guenther et al. 1993), and are defined as

$$C_T = \exp\frac{C_{T1}(T - T_s)}{R\,T\,T_s} \Bigg/ \left[1 + \exp\frac{C_{T2}(T - T_M)}{R\,T\,T_s}\right] \qquad (1.2), \text{ and}$$

$$C_L = \frac{\alpha C_{L1} L}{\sqrt{1+\alpha^2 L^2}} \quad (1.3)$$

where T (K) is leaf temperature, T_s (K) is the leaf temperature under standard conditions and R is the gas constant (8.314 J K^{-1} mol^{-1}). C_{T1} (95,000 J mol^{-1}), C_{T2} (230,000 J mol^{-1}) and C_{L1} (1.066) are empirical coefficients, and T_M (314 K) is the maximal leaf emission temperature. Data in use in current biogenic emission models/inventories, such as BEIS (Biogenic Emissions Inventory System), are based on laboratory emission experiments on aspen, eucalyptus, sweet gum and velvet bean leaves.

Basal emission is generally given as the emission at 1000 µmole photons cm^{-2} s^{-1} (400-700 nm = photosynthetically active radiation, PAR) and 30°C leaf temperature, and is based on plant biomass. Hence, leaf mass of emitting plant species is another major factor in estimating isoprene emissions of an area. A recent review (Pacifico et al., 2009) described current emission modeling efforts, which now also include correction terms for recent weather conditions and other stress factors affecting plant physiology, and therefore emissions. As incident PAR and ambient air temperatures are the dominant drivers of isoprene emissions, they are commonly the ones evaluated during local, canopy scale emission measurements, alongside the emitting leaf biomass (Baker et al., 2008; Guenther et al., 2000; Schade and Goldstein, 2001). To reduce the uncertainty from the much more complicated mixed sources in our heterogeneous study area and to show overall characteristics as the first measurements of isoprene flux in the middle of an urban area, we used the median isoprene flux to compare with the isoprene model

result. As in other studies, we used the normalization condition of 30°C of leaf temperature and 1000 μmol m^{-2} s^{-1} of PAR to determine basal emission rate (on an area basis).

In urban areas a complication is added to the emission and chemistry of isoprene because it is also emitted from anthropogenic sources, in particular as a tail-pipe emission (Borbon et al., 2001; Derwent et al., 1995; Reimann et al., 2000). As isoprene oxidation can contribute strongly to ambient ozone formation in the boundary layer, both its biogenic and anthropogenic emissions should be considered in emission inventories for metropolitan areas, especially those in violation or near violation of the National Ambient Air Quality Standard (NAAQS) for ozone. However, current emission inventories do not include isoprene as a tailpipe emission, and only consider biogenic emissions. While this is generally done through emissions modeling, there are few direct flux measurements for estimating and improving emission inventories in urban areas. However, considering the importance of ozone for public health in metropolitan areas (Balmes, 1993; Lang and Polansky, 1994; Sunyer et al., 1991), the contribution of isoprene to ozone formation (Li et al., 2007), and the at times poor performance of emission models due to inaccurate input data, direct measurements of urban isoprene fluxes are warranted. The recent urban flux measurement studies conducted by Velasco et al. (Velasco et al., 2005a), Langford et al. (Langford et al., 2009), focused mainly on urban anthropogenic VOCs. Although anthropogenic isoprene emissions are considered small compared to biogenic emissions (Reimann et al., 2000, Borbon et al., 2001), and

the density of isoprene emitting trees in urban areas is generally much lower than in forested areas, it may still be a significant or even major source of ozone formation (Chameides et al., 1988; Geron et al., 1995; Li et al., 2007). Indeed, a recent study of NMHC in US cities demonstrated that isoprene is the most dominant NMHC in nearly half of the cities (Baker et al., 2008).

To assist the State of Texas in assessing Houston's air pollutant emissions and state-wide traffic inventories, a tall flux tower installation was established. The objectives are to measure criteria pollutant and VOC fluxes on a semi-permanent basis to evaluate the appropriateness of current emission inventories, particularly for traffic emissions, to highlight shortcomings, and to outline necessary improvements in order to better air quality modeling and forecasting.

We introduce the geographical, meteorological and traffic conditions at the study site (north of downtown Houston) in Section 2, together with the methodology for the flux measurements using a REA technique and standard gas chromatography flame ionization detection (GC-FID). We also introduce the methodology to compare the EPA national emission inventory (NEI) with our measurement results by using geographic information system (GIS) software. In Section 3, we discuss the results of the diurnal variation of the concentration and flux of benzene, toluene, ethylbenzene and xylenes (BTEX), and show the estimated difference between our measured fluxes extrapolated to the county level with EPA NEI for Harris County, Texas. In Section 4, we discuss our

mixing ratio and flux measurements of isoprene and its oxidation products MACR and MVK, and reveal both anthropogenic and biogenic characteristics of those compounds by using footprint analysis and isoprene emission modeling, including an estimate of its local basal emission rate.

2. METHODOLOGY

2.1. Site description

To monitor neighborhood scale pollutant fluxes, a tall tower installation was established in a mixed land use area of Houston, north of downtown (Figure 2.1(a)). The tower's location (29°47'22'' N, 95°21'13'' W) is on private property of the Greater Houston Transportation Company (hereinafter called *Yellow Cab*). It is surrounded by residential areas in three directions (N, W and S; 28% of total area within a 1.5 km radius), two multi-lane commuter roads (West: Fulton St./Irvington Blvd.; East: Elysian/Hardy Rd.; roads cover 25% of total area in a 1.5 km radius), a light industrial area (East; 11%), and a park (West, Moody Park; 6%). The remaining land uses are dominated by commercial and public uses (5% each), and 'undeveloped land' (17%). Within the southern wind direction sectors of the site, prevailing during the study period, the residential land use (39%) and roads (31%) dominate.

The identified land uses (Figure 2.1(b)) generally correspond to four land cover classifications: 'high', 'medium', and 'low intensity developed', and 'open space' (USGS/NOAA classification at http://www.csc.noaa.gov/crs/lca/tech_cls.html), with >80%, 50-80%, 20-50%, and <20% impervious surface area, respectively. The southern sector, 1×2 km^2 from the tower, has a respective 38-57-4-1 percent distribution between these land covers, corresponding to an approximate 70% average impervious surface area, representative of a typical mixed-use urban region.

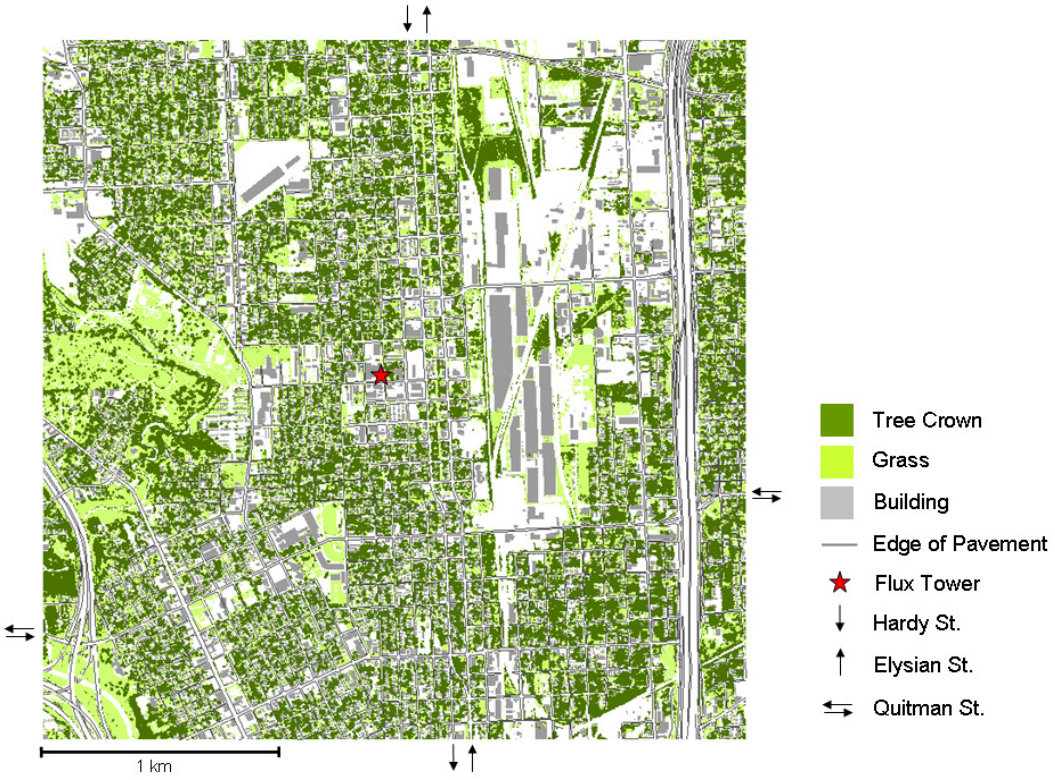

(a)

Figure 2.1. Site domain (3 km x 3 km centered on tower). (a) indicates the distribution of tree, lawn, building and roads, and (b) presents the land use with the wind rose during the summer study period.

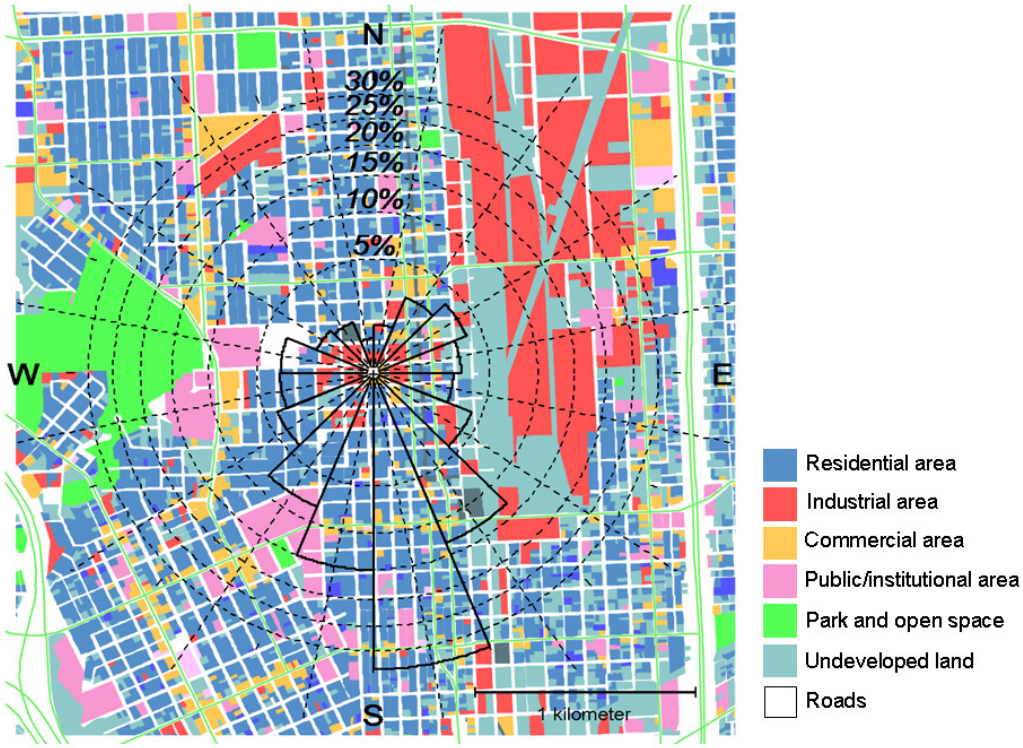

(b)

Figure 2.1 Continued.

2.2. Meteorological and traffic observations

Meteorological and micrometeorological observations during the study period in summer and winter are summarized in Figure 2.2.

In summer, lowest wind speeds occurred during the morning boundary layer transition period, then continually increased, maximizing during the late afternoon hours (~ 18:00) when the regional sea breeze is the strongest. Wind direction during the study period was dominantly from the south (Figure 2.1b), slightly affected by the afternoon sea breeze.

Non-southerly wind directions were caused by frontal passages and occurred only 29% of the time. We note that due to flat terrain and relative homogeneity of surface roughness elements at this site, half-hourly mean w values were not significantly biased under any wind direction except northerlies (influenced by the tower structure). Rotational angles were nearly always <5˚ (-0.5±2.2˚ (2 sd)), lending credibility to the sampling site. The highest temperatures during the measurement period, around 35˚C, were higher than normal for Houston as this time of year. In addition, June 2008 was also comparatively dry throughout east Texas, with Houston receiving only 40% of its normal precipitation that month (Texas Climatic Bulletin, http://www.met.tamu.edu/osc/tx/tx2008.html).

In winter, lowest wind speeds were also observed during the morning boundary layer transition period, then continually increased, maximizing during the late afternoon hours (~ 15:00) about 3 hours earlier than that in summer. Compared to dominantly (~ 70%) southerly wind directions in summer, winter wind direction showed about 24%, 10%, 44% and 22% of easterly, westerly, southerly and northerly wind conditions. The highest temperatures were around 28˚C, again higher than normal for Houston as that time of year, and the lowest ones were 3˚C during the winter measurements period. In addition, January and February 2009 were extraordinary dry throughout the entire states of Texas, with Houston receiving only 13% and 51% of its normal precipitation those months (Texas Climatic Bulletin, http://www.met.tamu.edu/osc/tx/tx2009.html).

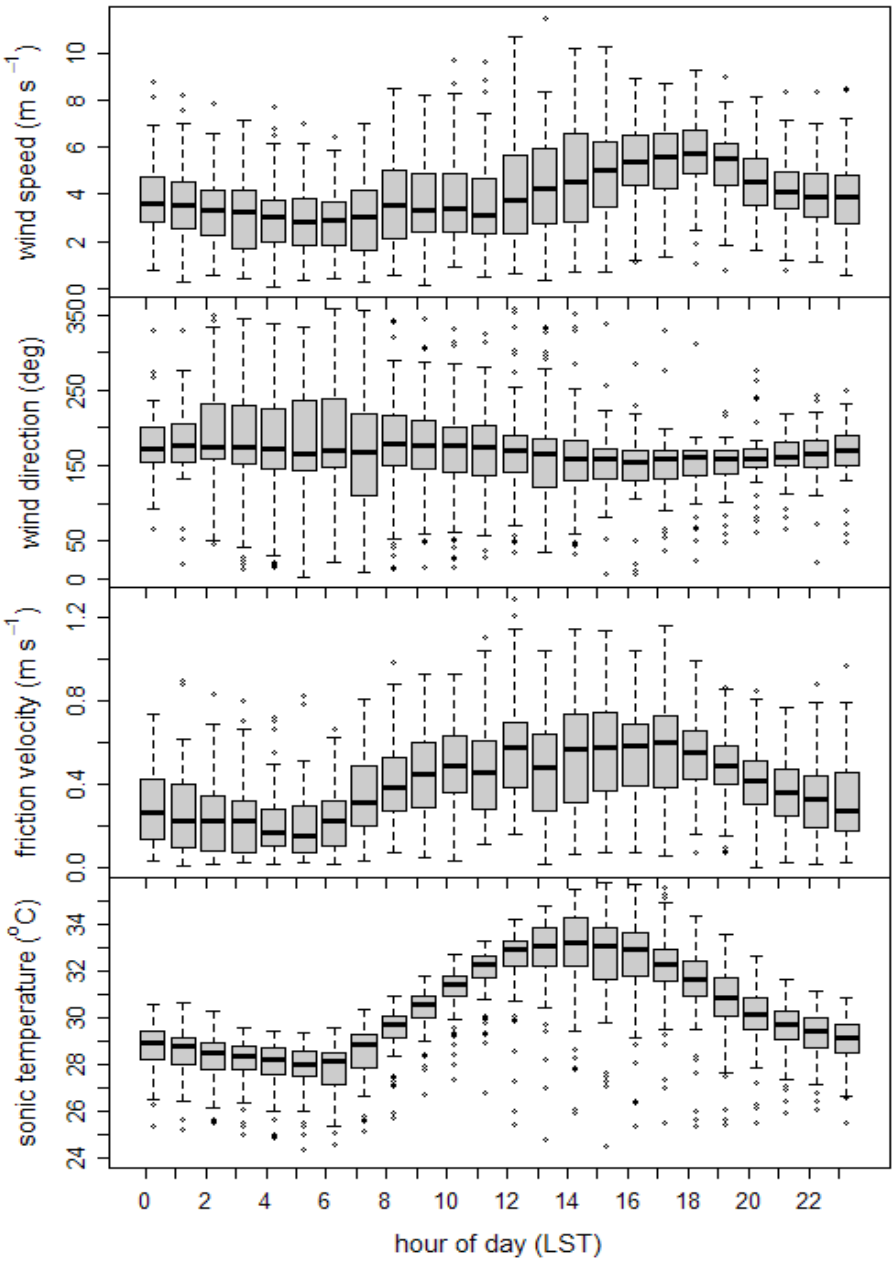

(a)

Figure 2.2. Boxplots of the diurnal variation of meteorological conditions during the 8 weeks in each summer (a) and winter (b) study period. Solid black bars are medians, gray boxes are inter-quartile ranges and whiskers represent 95% intervals. Individual data points lie outside 97.5% of the data. LST is Local Standard Time.

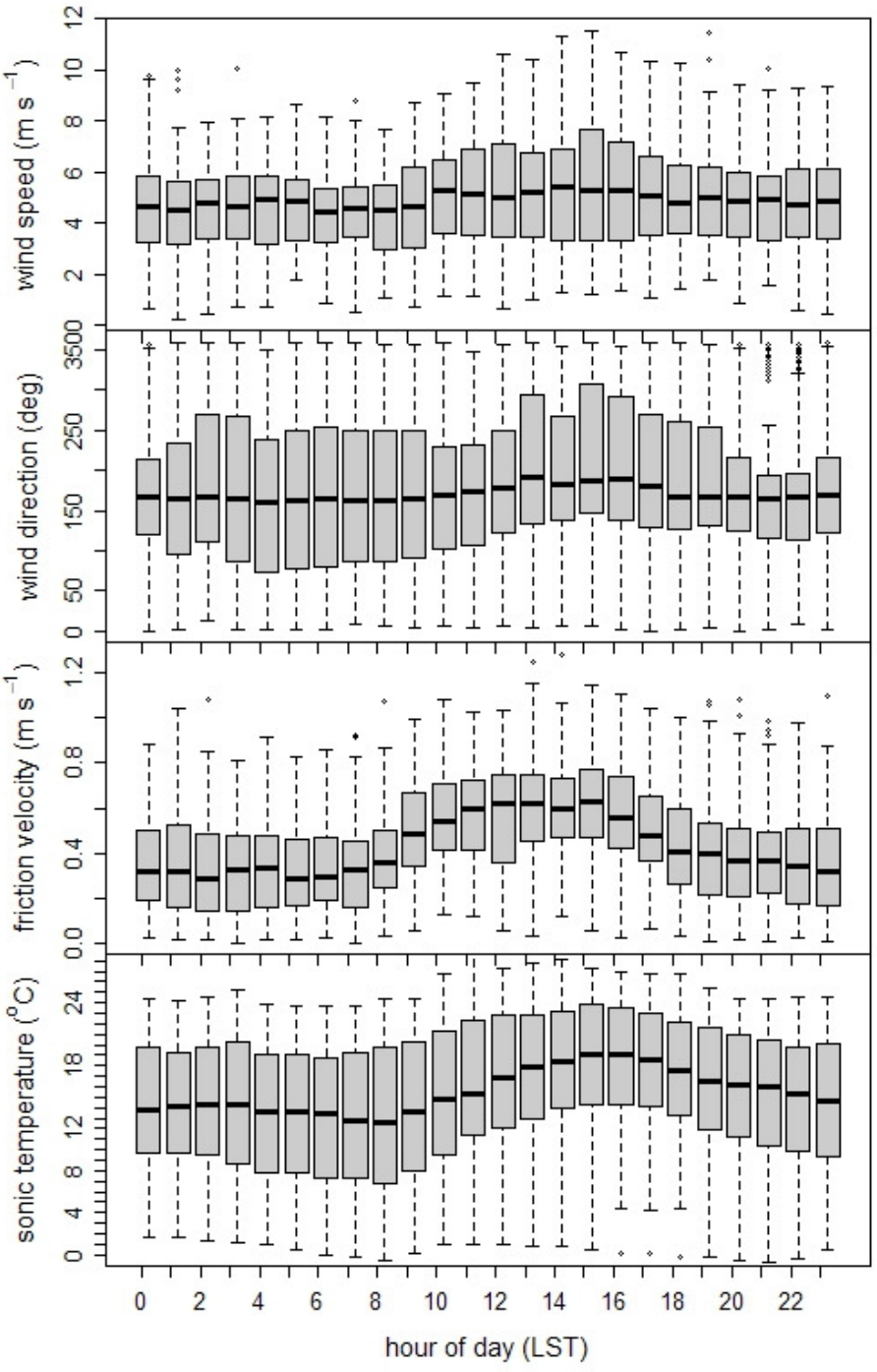

(b)

Figure 2.2 Continued.

Figure 2.3 shows average weekday and weekend raw traffic counts on Elysian/Hardy, and Quitman Streets (Figure 2.1(a)), which are the main commuter roads in southern sector of our study domain. The counts were obtained using rubber tube technology during a week-long period in January 2008 (courtesy of the Texas Transportation Institute, TTI), and demonstrate that the highest number of vehicles passed through the study domain during the morning and afternoon rush hours and that daytime weekend traffic remains at weekday levels, while higher traffic counts were observed during weekend nights.

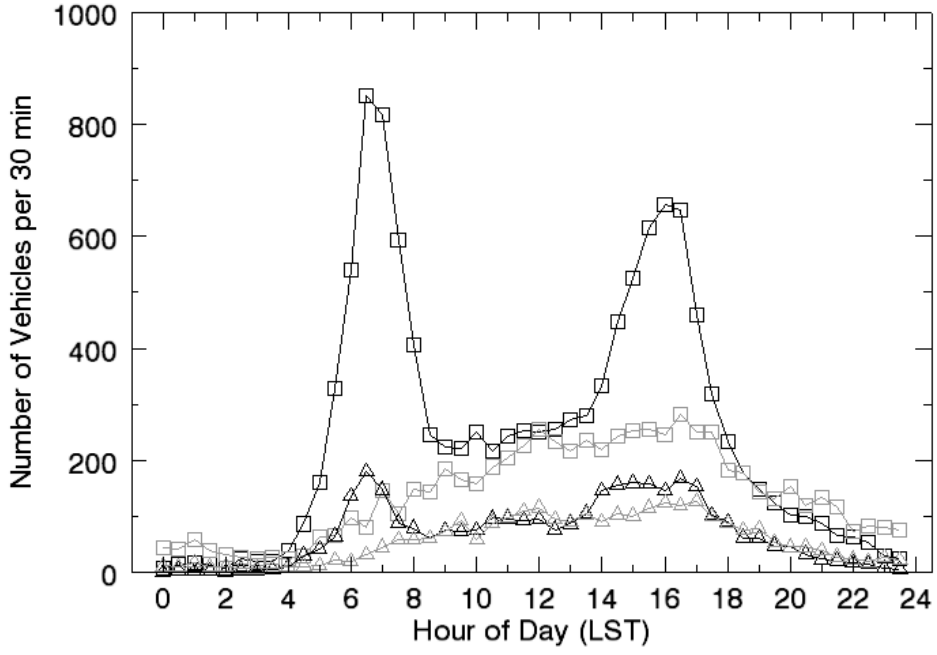

Figure 2.3. Average number of vehicles in 30 min intervals obtained on Elysian (north bound) and Hardy (south bound) Streets (squares), and Quitman Road (east/west bound; triangles) during January 16-21, 2008. Black and gray colors represent weekdays and weekend days, respectively.

2.3. Tree survey

To address isoprene emissions from biogenic sources, a local land cover and tree inventory survey was conducted. Figure 2.1(a) also shows land cover including tree distribution as determined from aerial photography around our study domain. Our tree survey indentified that oak trees account for about 27%, Sugarberry (*Celtis laevigata*) for 20%, Pecan (*Carya illinoensis*) for 11%, Chinese tallow (*Sapium sebiferum*) for 9%, Crape myrtle (*Lagerstroemia indica*) for 8%, and Green ash (*Fraxinus pennsylvanica*) for 5% of all trees in the study area. This distribution of tree species is biased towards oak and sugarberry as compared with the county level average distribution evaluated in 2005 (Houston's Regional Forest Report, http://www.houstonregionalforest.org/Report). The local oak species include live oak (*Quercus virginiana*, 26%), water oak (*Quercus nigra*, 23%), post oak (*Quercus stellata*, 23%), and willow oak (*Quercus phellos*, 16%) and white oak (*Quercus alba*, 6%).

2.4. VOC measurement system

2.4.1. Setup for sample flow path

Yellow Cab owns and operates a 91 m tall, triangular lattice communications tower (side length 60 cm) on the parking lot of its property. In May 2007, we installed meteorological sensors for T/RH and wind speed at four heights along the tower up to 60 m height above the ground. At the top installation height, a sonic anemometer for 3D wind speeds (CSAT3, Campbell Scientific Inc. (CSI), Logan, UT) controlled by a CR1000 data logger (CSI), radiation sensors, a combined wind speed and direction

sensor (model 034B, Met One Instruments Inc., Grants Pass, OR), and a ¼'' ID Teflon PFA tubing inlet next to the sonic anemometer constituted the flux measurement setup. Ambient air was sampled down through the PFA tube at approximately 15 L min^{-1} into an air-conditioned building next to the tower, where the GC-FID, a CO_2/H_2O analyzer (LI7000, Licor Biosciences, Lincoln, NE), and criteria air pollutant instrumentation for CO, NO_x, and ozone were located. A single, 2 µm pore size Teflon PFA filter at 3 m height on the tower removed particles from the air stream, and was changed once a week. For VOC subsampling, a Teflon-coated membrane pump extracted approximately 0.9 L min^{-1} from the main air flow via a ¼'' OD Teflon PFA tube with an inline ozone scrubber (KI coated glass wool). The air was pushed through a flow controller (PTFE/sapphire ball flow meter with needle valve; Cole-Parmer, Vernon Hills, IL) into the REA valve system.

2.4.2. Relaxed eddy accumulation (REA) setup

The REA method is an eddy covariance derived sampling method within the atmospheric surface layer, introduced for trace gases, for which no fast measurement sensor exists. Historically, the eddy accumulation method was proposed by Desjardins (Desjardins, 1972), then improved by Businger and Oncley (1990) to the relaxed eddy accumulation method. REA sampling is performed by two basic components: a fast-response (10 Hz) anemometer measuring the vertical wind speed, and a fast response valve system diverting sample air depending on the sign of the measured vertical wind

speed. For example, in the case of an updraft (positive vertical wind speed), the high-speed valve for updraft is opened, and the sample air enters the updraft reservoir.

Our REA system consisted of three fast-response two-way valves (model 100T2NC, Bio-Chem Valve Inc., Boonton, NJ; response time < 20 ms), one each for updraft and downdraft sampling, and a so called deadband for excluding sample air associated with small deviations of the vertical wind speed from its mean. The valves were driven by the data logger that acquired the instantaneous 3D wind speeds and computes a 5-min running average of the vertical wind speed (w) and its standard deviation (σ_w) (Schade and Goldstein, 2001), then buffered these values until this air arrived at the REA valve system. The associated lag-time (here: ~9 s), was computed offline from the maximum of the w-CO_2 covariance using the acquired 10 Hz data of CO_2 concentration by the CO_2/H_2O analyzer. Lag-time compared favorably with the estimated time from flow and volume (2.3 L) considerations. Lag-time fluctuations were found to be smaller than one second (2 sd) in our system, much shorter than the dominant reversal time between up and downdrafts, identified from power spectra of the binary REA command, of 25-75 s at night and 100-200 s during daytime.

Updraft and downdraft sampling was carried out when w exceeds mean(w) $\pm$ bσ_w , in which b is a discrimination factor introduced to vary the deadband size, and σ_w is the standard deviation of the vertical wind speed. Sample air enters either one of two 1 L Teflon bag reservoirs (SKC Gulf Coast Inc., Houston, TX), connected via $^1/_8$" OD PFA

tubing, for 30 minutes at the top of the hour. We used a b factor as high as 1.1 corresponding to a deadband size of almost 80% of the total sample to maximize the concentration differences of emitted VOCs in the up and downdraft samples. At this setting, a sample size of approximately 3 L per 30-min sampling period (≤3 min (10%) of sampling each per reservoir) was achieved. To avoid overfilling the 1-L Teflon bags, the air was nearly simultaneously transferred to the GC preconcentration units. Figure 2.4 shows a schematic of our REA system. It is unique in the sense that it can maximize the updraft-downdraft concentration difference, thereby increasing flux measurement sensitivity, without compromising sample size, the typical limitation in most previous setups.

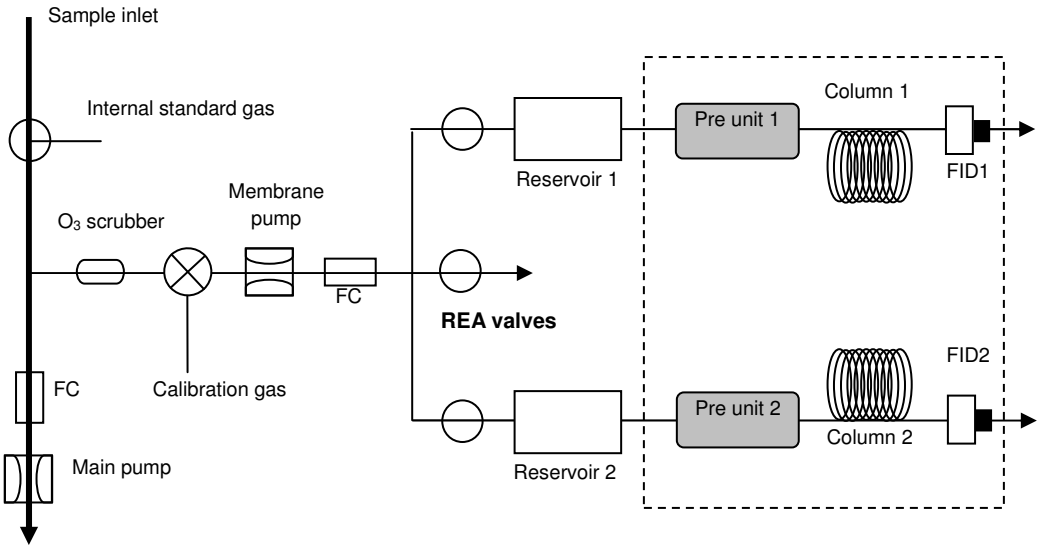

Figure 2.4. Schematic of REA-GC-FID system. The dashed line box indicates the parts of the GC-FID system. The preconcentration units ("Pre Unit") are described in more detail in the figure on page 27.

From the REA system data each VOC flux (F) is calculated using

$$F = \beta\sigma_w (C_{up} - C_{down}) \qquad (2.1).$$

The β factor is a unitless coefficient, which in ideal atmospheric turbulence conditions such as over flat, homogenous terrain has a value of approximately 0.58 (Katul et al., 1996) when no deadband is used. It is generally assumed to be constant, but commonly calculated from measurements of sensible heat flux and the virtual mean air temperatures that correspond to the sampled up and downdrafts (Businger and Oncley, 1990; Katul et al., 1996; Schade and Goldstein, 2001) when a deadband is used. The standard deviation of the vertical wind speed over the 30-min collection period is σ_w, and C_{up} and C_{down} are concentrations of each compound of interest in the up and down reservoirs, respectively, measured by GC-FID.

The REA method used here bears an additional uncertainty through the need to calculate the flux correction factor β. The β-value is thought to depend on atmospheric stability (Ammann and Meixner, 2002; Andreas et al., 1998; Milne et al., 2001) but is generally calculated from the wind speed measurements inverting Eq. (2.1) such that

$$\beta = \frac{\overline{w'T'}}{\sigma_w (\overline{T}_{up} - \overline{T}_{down})} \qquad (2.2)$$

where the primes denote deviations from the respective mean values. Large uncertainties are introduced into this calculation when the dominator in Eq. (2.2) approaches 0, namely during near neutral atmospheric stability, commonly observed during times when the sensible heat flux changes sign in the morning and evening hours. Baker and

coworkers (1992), Bowling et al. (1998) and Schade and Goldstein (2001) discarded calculated β values when sensible heat fluxes were small. Here, we decided to use a fixed β corresponding to the median of all half-hour values calculated using Eq. (2.2); here: 0.355.

A closer evaluation of the sampling scheme revealed that the chosen 5-min average mean and standard deviation was too short to be representative of the turbulence at 60 m agl. As a consequence, the β calculation following Eq. (2.2) overestimated β by 15-20 % as compared to a calculation using the a-posteriori known 30-min mean(w) and standard deviation together with eddy covariance heat flux. The "correct" β was calculated to be 0.3, close to the value 0.27 forecasted using Businger and Oncley's equation (Businger and Oncley, 1990) (Figure 2.5). However, there is also the possibility of potential bias in concentration difference between up and downdrafts. We used Eq. (2.1) to estimate a REA heat flux using the "correct" β together with our actually sampled temperature difference in the up and downdrafts, and compared it to the eddy covariance heat flux (Figure 2.6). We found that our sampling scheme may have underestimated the concentration difference by 25±5% (from a bivariate regression). Although the biases nearly cancel each other, our flux values are likely underestimates on the order of 10% (note that biased sampling will always lead to fluxes lower than the "correct" fluxes).

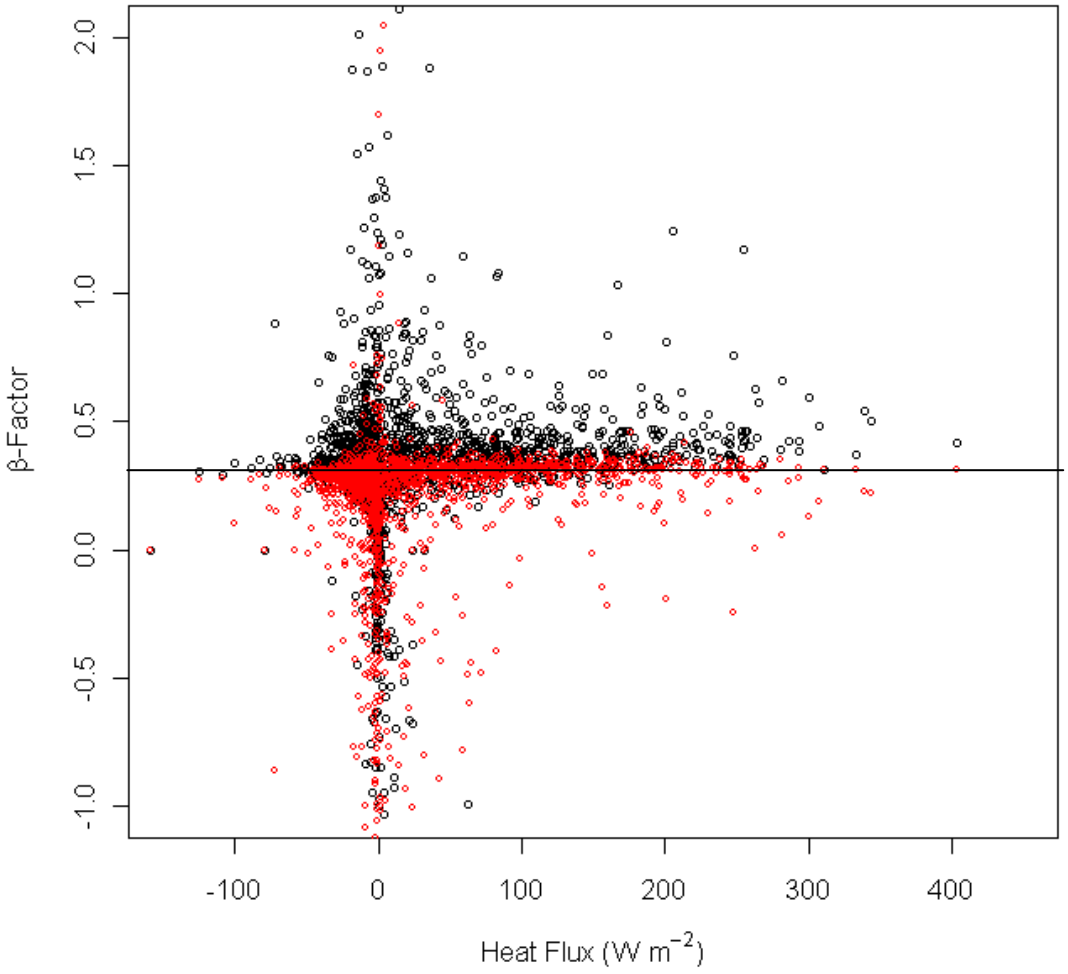

Figure 2.5. β-factors as a function of heat flux (some negative values omitted from graph). Black points are based on our sampling scheme, red points are from a calculation using 'perfect REA sampling' (see text). Note that median (β) for the red points (0.3) is close to the Businger and Oncley (Businger and Oncley, 1990) prediction of 0.27 for a discrimination factor of 1.1.

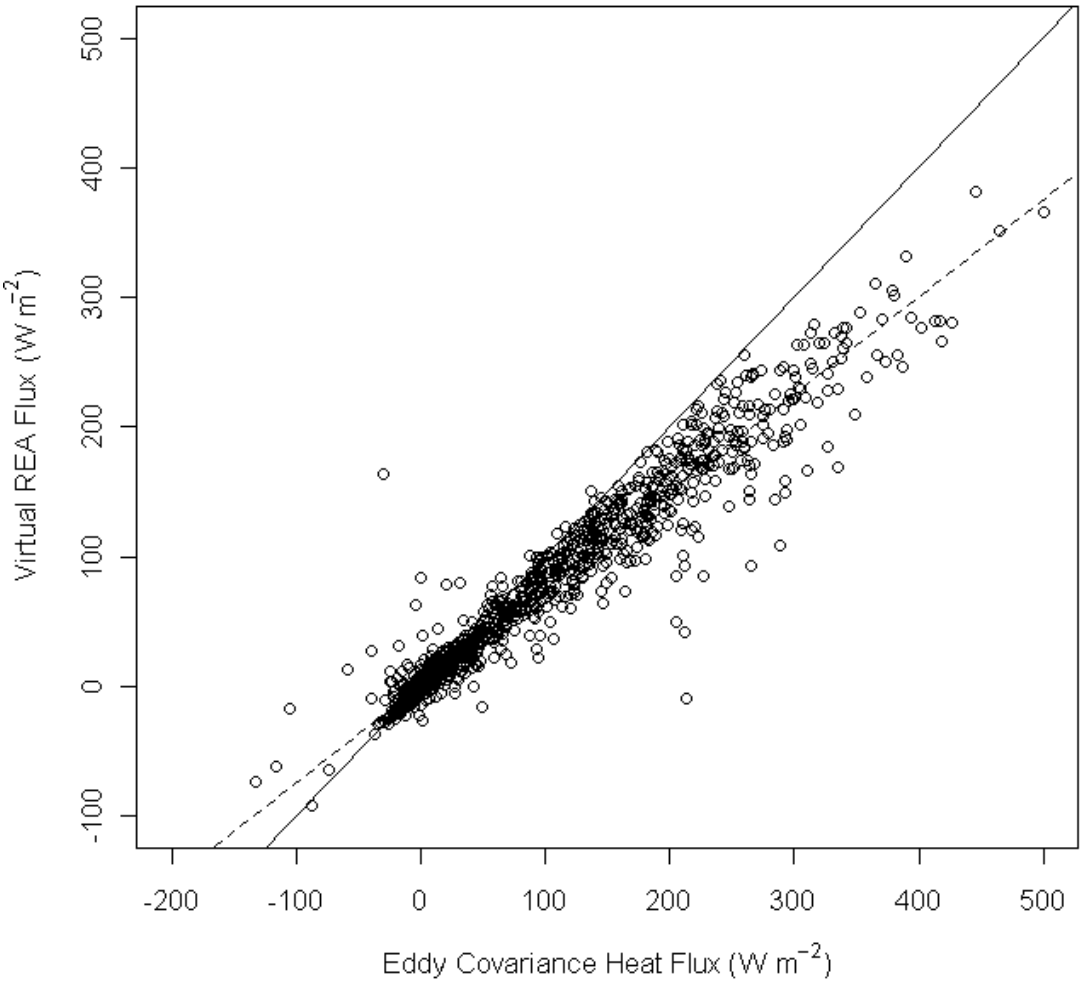

Figure 2.6. EC versus virtual REA heat fluxes. The solid line is a 1:1, the dashed line the regression from a major axis regression (slope = 0.75).

2.4.3. GC-FID analysis

The GC-FID system consisted of a portable SRI model 8610 C with dual channel setup (SRI Instruments, Torrance, CA). Each channel had a preconcentration unit, a capillary

column with a guard column, and an FID fueled by zero air and hydrogen from onsite generators (AADCO model 737-1 and Matheson Tri Gas model HYC-SEPG-100). Figure 2.7 depicts the preconcentration unit. A single, software-controlled pump aspirated sample air from the Teflon bags into one each updraft and downdraft preconcentration unit seven to eight minutes offset from the sample acquisition interval for a total time of 30 minutes. The sampling flow rate was controlled by two flow controllers (AALBORG, Orangeburg, NY) to 100 mL min^{-1}. Each preconcentration unit consists of a $^{1}/_{8}$'' OD, 10 cm length Silcosteel® adsorption trap filled with 60/80 mesh Carbopak-B (50%), Carbopak-X (30%) and Carboxen 1000 (20%) (all Supelco, PA), and was encapsulated in a heater block. After sampling was complete and the GC was ready, each valve rotated in turn, so that during the first 12 seconds of the GC operation, the carrier gas swept each trap consecutively to remove oxygen. Both samples were then thermally desorbed directly into one each 0.53 mm ID Rtx-MXT624 column via 10-port Valco® valves and $^{1}/_{16}$'' OD Silcosteel® tubing 15 minutes after sample collection ended (Figure 2.7).

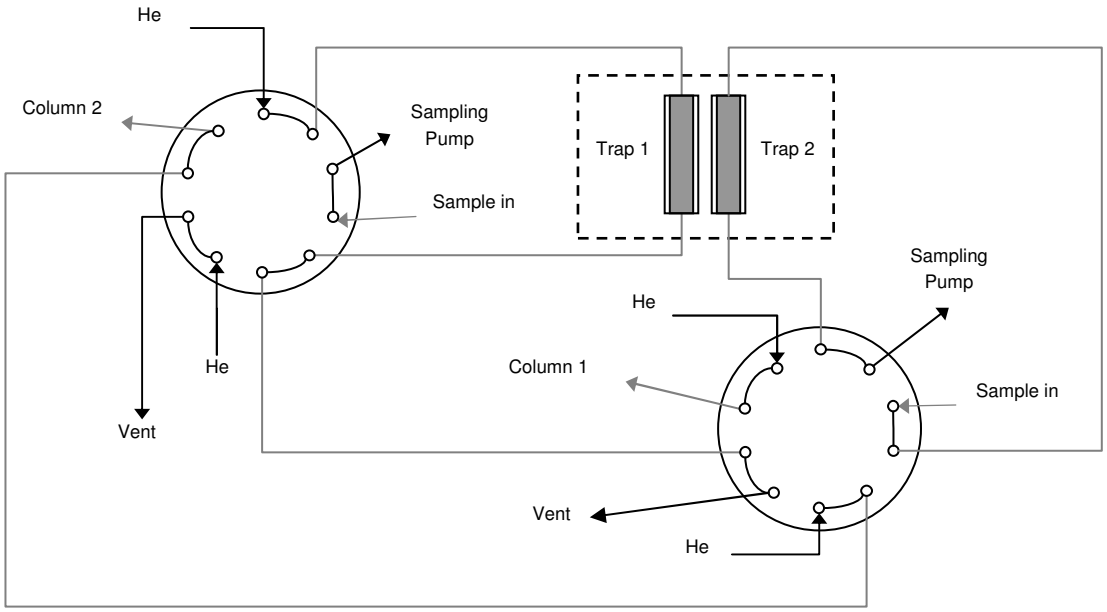

Figure 2.7. Depiction of the preconcentration unit (10-port valves, traps and sampling pumps) as part of the SRI gas chromatograph. All lines in contact with the sample are Silcosteel tubing (grey lines). Both vents are metered with a needle valve to control the He carrier gas flow rate during the trap purge. Dashed line box indicates the heater blocks.

Chromatographic data acquisition and GC control were carried out via PeakSimple software (SRI Instruments, Torrance, CA). The GC oven temperature program was set to hold at 30°C for 10 minutes, then ramp at 4°C/min to 120°C, then ramp again at 20°C/min to 215°C. After an additional 9 minutes holding time, the temperature was decreased till the end of the run. The initial column head pressure was set at 0.5 kPa (7 psi), then held or ramped in order to provide a near constant flow through the MXT columns. Raw chromatographic data were reanalyzed offline for consistency using PeakSimple set to output area counts to an ASCII file.

2.5.Quality control

2.5.1. Zero and channel intercomparison tests

Zero air sampling was initiated by the data logger every 30 hours by turning a three-way valve located in front of the sample acquisition pump (Figure 2.4), changing the sample flow from ambient air to zero air provided by the zero air generator. Aside from these regular zero measurements, zero air sampling also commenced during rain events. Generally, the zero air samples showed negligible contamination respectively carry-over for all components of interest (Figure 2.8). When contamination was present, we often found significant abundances for all commonly measured VOCs, which was nearly always traced to a leak in one or both of the Teflon sample bags. When contamination was present, affected measurements were corrected for the leakage until the respective reservoir's leak was fixed.

As the two analytical channels from each REA valve down to the FID via a pump, a bag reservoir, a preconcentration unit, and a column, were not likely to operate identically, a channel intercomparison was done every 30 hours with a 10 hour offset from zeroing by opening and closing the updraft and downdraft valves simultaneously, thereby acquiring identical samples into the bags. The comparison of these samples allowed us to monitor any channel offset as caused by the complete sampling and analysis system (Schade and Goldstein, 2001). We selected 32 single hydrocarbons out of these samples to determine an average channel ratio assuming the updraft channel is the "correct" one, then multiplied the downdraft channel with a correction factor determined from the internal

standard (IS) measurements. For example, before applying this intercomparison correction, the average slope of channel 1 to 2 was 0.92 for the IS, and 0.89 for toluene. After correction, the channel ratio for toluene was near 1.0 (Table 2.1).

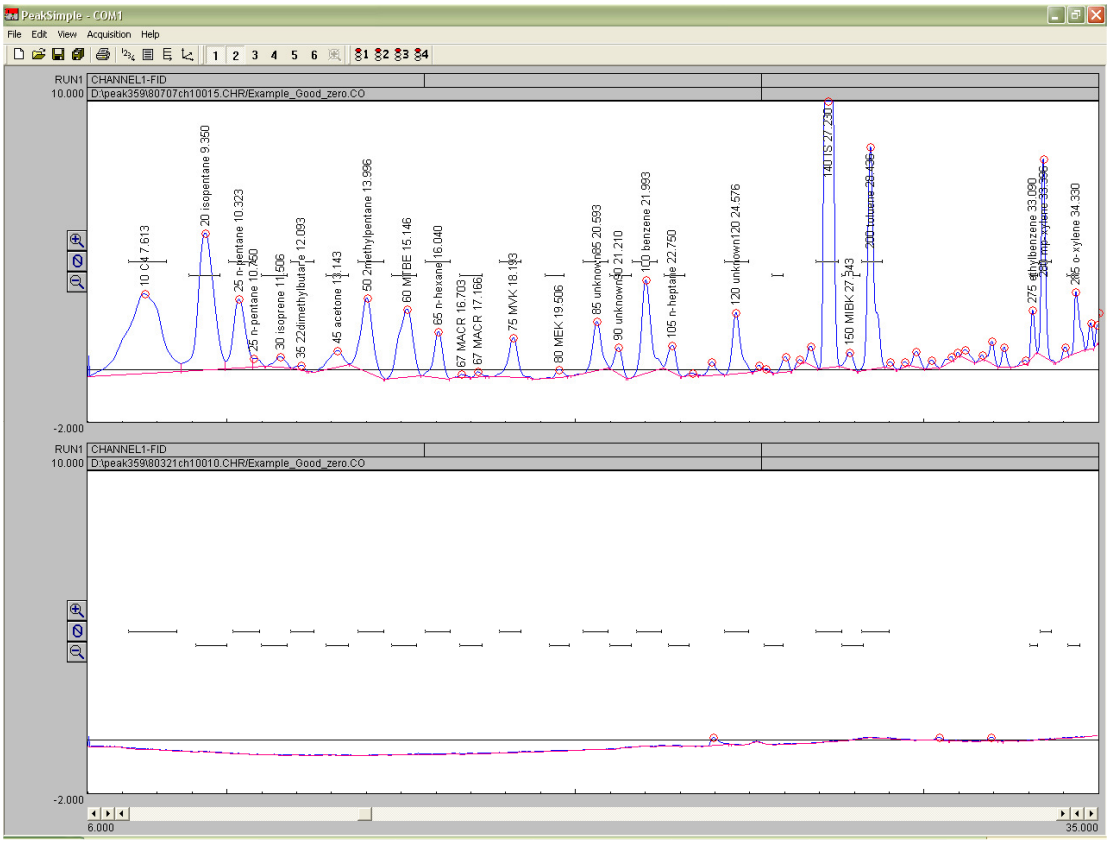

Figure 2.8. Example chromatograms of ambient air (upper panel) and zero air (bottom panel).

Table 2.1
Correction factors of slope and correlation coefficient (R) before and after channel intercomparison. (Assuming "up-channel" is the correct one, plotted on x-axis).

	Before correction		After correction	
	Slope	R	Slope	R
Benzene	0.91	0.98	0.99	0.98
Toluene	0.90	0.97	0.98	0.97
Ethylbenzene	0.90	0.98	0.98	0.98
m,p-xylene	0.95	0.95	1.03	0.95
o-xylene	0.93	0.98	1.01	0.98

2.5.2. Quantification

The GC-FID system was tested in the laboratory to determine optimal sample size, channel differences, breakthrough characteristics of the adsorbent traps, and optimal chromatographic separation. Because the traps operated at room temperature, C_2 hydrocarbons were not, and C_3 hydrocarbons were incompletely trapped. C_4 hydrocarbons experienced minor breakthrough at high ppb-mixing ratios and incomplete separation, but all higher hydrocarbons ($\geq C_5$) tested were trapped completely up to high ppb mixing ratios (>500 ppb). The detection limit (S/N=3) for n-hexane as determined from calibration curves using a 15.8 ppm standard (Scott Specialty Gases, Plumsteadville, PA) and based on a minimum area count of 0.5 as measured with PeakSimple, was 6 ppt for a 3 L air sample. BTEX detection limits are similar based on the uniform carbon response of the FID. In laboratory we injected an n-hexane compound mix in nitrogen (including n-propane at 15.6 ppm, n-butane at 15.6 ppm, n-pentane at 15.7 ppm, n-hexane at 15.8 ppm and n-heptane at 15.8 ppm) three times at each volumes of 2 ml, 4 ml, 6 ml and 8 ml, using a 10 ml min^{-1} flow controller. Figure

2.9 presents an example of a resulting calibration curve between peak areas measured by Peaksimple and concentration of the n-hexane standard.

Compound identification is based on retention time as compared to single or multi-species standards using injection into real air and zero air samples. Laboratory calibrations suggested a repeatability of 6% relative standard deviation (RSD) at 15.8 ppb determined by injecting the IS three times at each amount of 2 ml, 4 ml and 8 ml at a time, and an accuracy of hydrocarbon measurement of 11.6% including the error of standard gases (10%), flow controllers (5%), and calibration error (3% from the determination R^2 in Figure 2.9). Due to the high linearity and carbon proportionality of the FID (Ackman, 1968), we used an IS calibration in routine daily operations. A weighted response factor (RF_i) for each compound was calculated (Ackman, 1964), and the IS's response factor was calculated from dilutions of the ppm-level IS into the main tower line. We used 3-methyl-heptane as the IS as it was (i) not naturally abundant at this measurement site, (ii) well separated on this column, and (iii) fully trapped on and released from the used preconcentration traps.

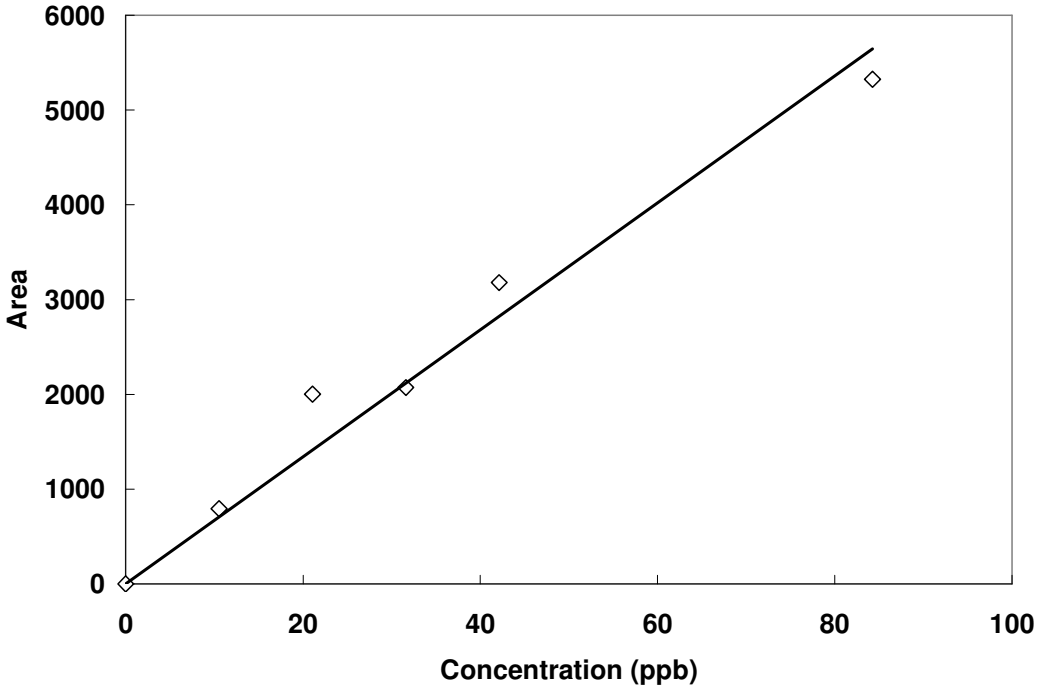

Figure 2.9. An example of a calibration curve between concentrations and peak areas. The best fit linear equation is: (area) = 67.0 · (ppb) with a determination coefficient (R^2) of 0.97. Diamonds indicate individual standard injections.

For the data presented here, the response factor of the IS (RF_{IS}) was calculated based on more than 706 samples produced by varying the concentration of the IS via three dilution ratios within several weeks of instrument operation, and determining RF_{IS} from the regression equation from peak area versus concentration for each channel. The regression's RSD of 10.2% may be interpreted as the complete system's precision, which is apparently dominated by the GC-FID method reproducibility. Individual hydrocarbon response factors (RF) were determined either from standard mixes, or mass-%C of the hydrocarbon relative to the internal standard compound (RF_m). Lamanna and Goldstein (1999) showed that the ratio of RF/RF_m is generally close to 1.

Here, we assume that RF_m is representative of the correct response factors and we used the derived RF from mass %C relative to the IS to quantify all hydrocarbon species measured in the field (Table 2.2).

Table 2.2
Quantification parameters of BTEX compound.

Compound	Blank, ppbv	Derived RRF_i	Ratio RF_{IS}/RRF_i
Benzene	<LDL	0.823	0.010
Toluene	<LDL	0.950	0.009
Ethylbenzene	<LDL	1.076	0.008
Xylenes	<LDL	1.076	0.008

Here, <LDL denotes below least detectable limit; RRF_i denotes mass %C weighted response factor for the individual compounds relative to IS (3-methylheptane); RF_{IS} is the response factor of IS.

2.5.3. Footprint analysis

To further investigate VOC emission origins, we calculated the flux footprint (FFP) area "climatology" to determine the spatial distribution of isoprene emission sources during the morning rush hour and daytime hours, respectively. We used the analytical footprint model of Kormann and Meixner (Kormann and Meixner, 2001) as part of the EdiRe flux analysis software (University of Edinburgh, UK). The input parameters to the model are measurement height, wind direction, wind speed, standard deviation of crosswind variation, friction velocity, and Monin-Obukhov stability (z/L). Generally, the model output is a map of source probability density, which, in this case, was chosen to be of 30×30 m^2 grid density out to 3 km distance from the tower. There are several limitations to this analysis that have to be considered: (i) although the model compares reasonably

well with a more sophisticated Lagrangian stochastic particle trajectory model (Kljun et al., 2004; Kljun et al., 2002), it does poorer under neutral to stable atmospheric conditions, and occasionally returns integrated source areas of less than 80%; and (ii) the analytical model was not designed for heterogeneous urban surface areas and therefore at best returns a distribution representative of fluxes at the displacement height level. In our urban case, we determined that the surface layer turbulence is highly consistent with previous urban measurements (Roth, 2000), and our measurement height of 60 m is approximately six times the displacement height and therefore well outside the roughness sublayer. Hence, we conclude that the footprint model output should present a qualitatively correct picture of surface sources.

2.5.4. Comparison to EPA NEI

To compare our data to the EPA NEI, the county level emission inventory data was retrieved from the EPA chief pages (http://www.epa.gov/ttn/chief/eiinformation.html), which provide categorized criteria and hazardous air pollutant emission data for different years online. Only the emission categories ‘nonpoint’ and ‘onroad’ were used in the comparison as their definitions correspond directly with the identified sources in the study domain. ‘Onroad’ emissions include both tailpipe and evaporative emissions from vehicles, while ‘nonpoint’ emissions include evaporative sources such as commercial and industrial solvent uses. EPA’s SCC code listings, representing different sources categories, were used to select only those ‘nonpoint’ sources likely or potentially present in the study area.

We assumed that measured emissions can be extrapolated to the county level through upscaling by applying the land cover data set, which implies similar traffic composition, traffic speeds, and land cover as in our footprint throughout the county. We used ArcGIS (ESRI, Redlands, CA) with Texas 2005 land cover data from the Gulf Coast Land Cover study (http://www.csc.noaa.gov/crs/lcd/gulfcoast.html; NOAA Coastal Services Center) consisting of 22 categories (Table 2.3). Only the two urban land cover categories 'high' and 'medium' intensity developed', covering 1,344.21km^2 in Harris County (total county area is 4,530.07 km^2), were used (see section 2.1). The BTEX flux extrapolation assumed that the measured flux is coming only from these land cover categories in the footprint and that the footprint is representative. The extrapolation used overall median fluxes as well as individual median daytime versus nighttime and weekday versus weekend fluxes. The potential systematic error from this areal extrapolation was estimated to be a factor of two by considering extreme contributions from the two urban land cover categories, such as 100% of emissions from only the 'high intensity developed' category in the footprint, at our site versus the whole county.

Table 2.3
Land cover categories in the GIS data base.

Class name (Harris County only)	Grid pixel counts (30 x 30 m^2)	Area (km^2)	Contribution (%)
High Intensity Developed	468645	435.4	9.3
Medium Intensity Developed	1024927	952.2	20.4
Low Intensity Developed	663421	616.3	13.2
Developed Open Space	525719	488.4	10.4
Cultivated	143387	133.2	2.8
Pasture/Hay	668186	620.8	13.3
Grassland	189646	176.2	3.8
Deciduous Forest	189547	176.1	3.8
Evergreen Forest	302753	281.3	6.0
Mixed Forest	144035	133.8	2.9
Scrub/Shrub	128081	119.0	2.5
Palustrine Forested Wetland	312399	290.2	6.2
Palustrine Scrub/Shrub Wetland	60752	56.4	1.2
Palustrine Emergent Wetland	46686	43.4	0.9
Estuarine Forested Wetland	102	0.1	0.0
Estuarine Scrub/Shrub Wetland	404	0.4	0.0
Estuarine Emergent Wetland	9032	8.4	0.2
Unconsolidated Shore	10889	10.1	0.2
Bare Land	39179	35.4	0.8
Water	95659	88.9	1.9
Palustrine Aquatic Bed	9482	8.8	0.2
Estuarine Aquatic Bed	482	0.4	0.0
Total	5033413	4676.2	100.0

3. RESULTS OF MIXING RATIO AND FLUX OF BTEX AND ESTIMATE OF EPA NEI

3.1. BTEX in summer

We discuss results of measured concentrations and fluxes of the BTEX species in summer, commonly associated with car traffic exhaust emissions. Results are presented for the period of May 22 –July 22, 2008 (day of year (DOY) 143 – 204)). For quality assurance, only flux data acquired under sufficiently turbulent atmospheric conditions, in this case a friction velocity (u*) exceeding 0.20 m s^{-1} were retained. About 70% of all data were sampled under southerly wind conditions, and only results for the southern directions (135 - 225°), comprised of a largely uniform residential land use, were chosen for analysis, avoiding potentially biased conditions due to single large emitters. The u* filter removed 33% of the total data. Further filtering using the stationarity criterion (Foken and Wichura, 1996) on simultaneously measured CO_2 and CO concentrations removed an additional 6% of the data.

3.1.1. BTEX concentration

The observed BTEX concentration patterns (Figure 3.1) exhibited typical trends expected in an urban area: a weekday morning rush hour peak followed by a drop and lower daytime abundances, alongside lower concentrations without a significant rush hour peak during the weekends. Early morning minima occurred around 3:00 local standard time (LST, used for all times hereafter). Daytime BTEX minima generally

occurred in the afternoon, likely a result of reduced emissions into the maximum boundary layer (BL) height at that time. Typically, the second rush hour period (14:00 – 18:00) was not observed until 23:00 – 24:00 as a result of BL dynamics. Under typical urban heat flux conditions, the mixing layer height is kept high throughout the afternoon and evening hours, preventing surface layer VOC concentrations to accumulate fast. The observed late evening maximum was very similar to that observed in Dallas (Qin et al., 2007).

In Table 3.1, we compare our concentration results to earlier studies in Houston (Berkowitz et al., 2005; Reiss, 2006; Smith et al., 2007). For representativeness, values calculated from all observed wind directions are shown. At Yellow Cab, we observed slightly lower median values of BTEX compounds except xylenes compared to the Deer Park site (Smith et al., 2007), most likely as a result of that site's nearness to petrochemical sources in the Houston Ship Channel. Among CATMN and PAMS site data between 1997 and 2004, analyzed by Reiss (2006), we focus on the Aldine site for comparison, since it is relatively far from the petrochemical industrial sources and surrounded by similar land uses than our site. We included a comparison of toluene and m,p-xylenes with the measurements at the Williams Tower in west Houston (Berkowitz et al., 2005), since those measurements were also obtained at a higher elevation.

Table 3.1
Summer BTEX mixing ratios in Houston for all wind directions (in ppb = nmol mol^{-1}; LDL = lower detection limit).

	Max.	Mean	Median	Min.
Benzene				
This study [a]	2.38	0.51	0.36	0.09
Deer Park [b]	1.71	0.64	0.46	0.12
Aldine [c]		0.42		
Toluene				
This study	2.73	0.72	0.54	<LDL
Deer Park	1.44	0.60	0.59	0.25
Williams tower [d]		0.55		
Ethylbenzene				
This study	0.50	0.11	0.08	<LDL
Deer Park	0.23	0.12	0.10	0.03
Xylenes				
This study	2.57	0.61	0.45	0.09
Deer Park	1.03	0.45	0.39	0.12
Williams tower		0.39 [e]		

[a] values for all wind directions.
[b] (Smith et al., 2007).
[c] recalculated value based on the summer/winter ratio and the annual trend at the Aldine site (Reiss, 2006).
[d] recalculated value based on the reactivity (Berkowitz et al., 2005) and the OH reaction rate constant (Atkinson, 1994).
[e] mean value of only m and p-xylenes.

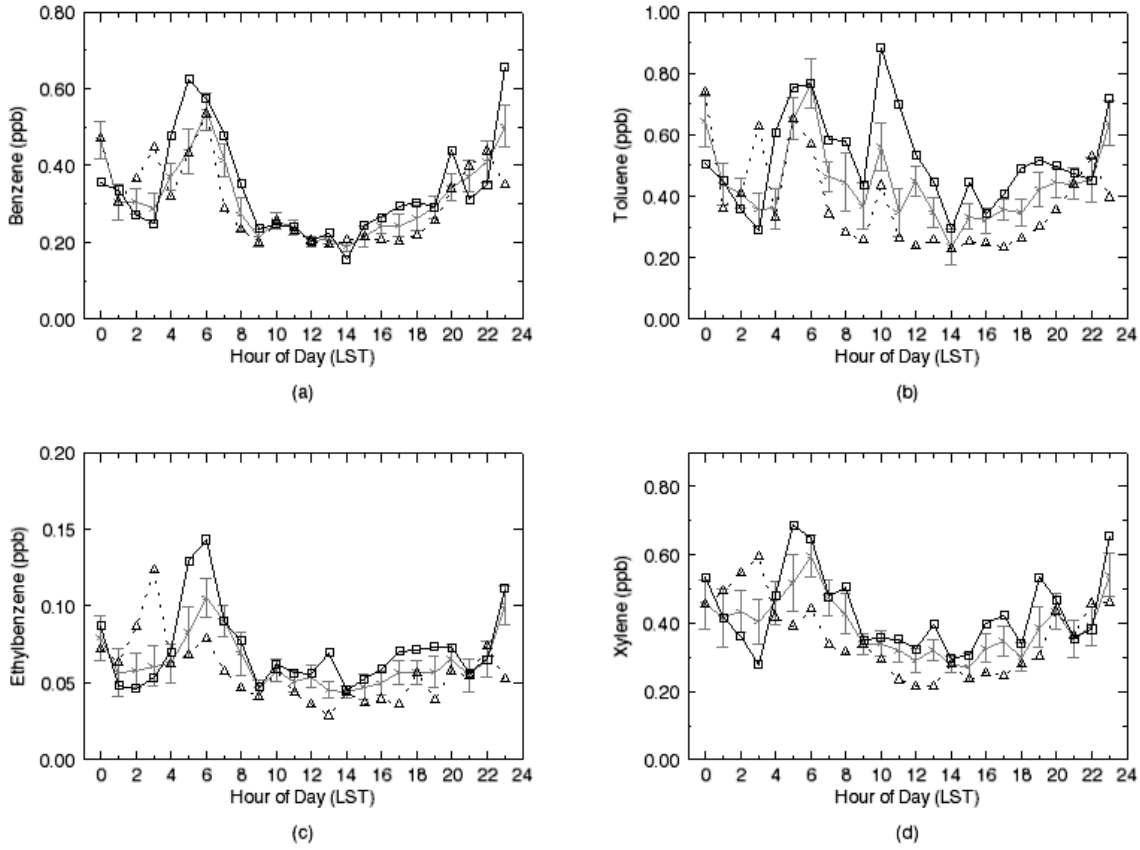

Figure 3.1. Diurnal median concentrations of BTEX compounds in updrafts (southern wind sector only) during the summer campaign. The thick line with error bars (standard error) shows all-day medians; the square-solid and the triangle-dotted lines show weekday and weekend data, respectively.

3.1.2. Fluxes of BTEX (summer)

Median diurnal flux variations of the BTEX species are shown in Figure 3.2, with statistics listed in Table 3.2. Overall, we found fluxes of toluene to dominate BTEX flux, followed by xylenes, benzene and ethylbenzene. All BTEX compounds showed a maximum during the morning rush hour on weekdays. A weak weekend evening peak

(higher than during weekdays) was observed, likely due to increased car traffic (Figure 2.3). During weekdays, toluene, xylenes, and ethylbenzene also showed dominant working hour (09:00 – 14:00) peaks, creating clear weekday-weekend differences not observed for benzene. This strongly suggests the contribution of evaporative emissions to the total fluxes in this area, which we discuss in section 3.3. Table 3.3 shows flux statistics separated into weekday versus weekend, and day versus nighttime. It shows that daytime weekday values were higher than weekend values (except for benzene), while nighttime weekend values were not significantly different. In comparison with the studies carried out in urban Mexico City, Mexico by Velasco et al. (2005a), and in Manchester and London, UK, by Langford et al. (2009; 2010), our mean value of toluene flux was approximately 1.4 times lower and approximately 1.2 – 2.1 times higher, respectively. Comparing the traffic counts around our site (~5,500 vehicles per day) to those acquired in Mexico City (>80,000), Manchester (~13,000), and London (>10,000), this result may be explained by a higher traffic density in Mexico City, but is inconsistent with the results obtained in the UK cities. Higher evaporative emissions likely contribute to this discrepancy, as are differences in car fleet composition and emission standards.

Table 3.2
Statistics for the measured fluxes of BTEX (in mg m^{-2} h^{-1}) for southern wind direction only in summer.

	Benzene	Toluene	Ethylbenzene	Xylenes
Max	1.69	6.23	1.35	6.64
Mean	0.17	0.58	0.07	0.56
	0.12[a] 0.15 [c]	0.28[a] 0.83[b] 0.68 [c]		
Median	0.17	0.44	0.05	0.41
SD	0.24	0.75	0.12	0.66
N	572	562	568	562

[a] measured in Manchester, UK (Langford et al., 2009)
[b] measured in Mexico City, Mexico (Velasco et al., 2005a).
[c] measured in London, UK (Langford et al., 2010)

Table 3.3
Day/night and weekday/weekend median values of the measured BTEX fluxes (Unit: mg m^{-2} h^{-1}). Daytime is 6:00 to 17:00 and nighttime 18:00 to 5:00 LST.

Compound	Daytime		Nighttime	
	Weekday	Weekend	Weekday	Weekend
Benzene	0.20	0.20	0.09	0.17
Toluene	0.70	0.48	0.33	0.31
Ethylbenzene	0.07	0.06	0.04	0.05
Xylenes	0.62	0.37	0.34	0.28

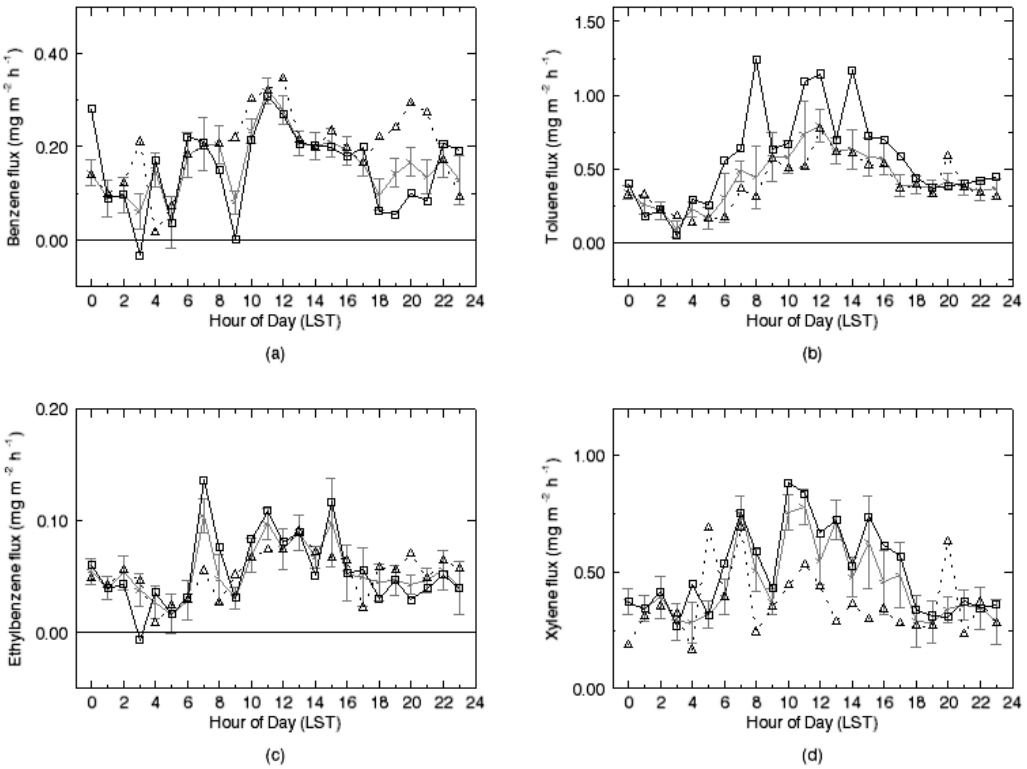

Figure 3.2. Same as Figure 3.1, but for fluxes of BTEX species.

3.2. Mixing ratio and fluxes of BTEX in winter

We show the results of measured concentrations and fluxes of the BTEX species during winter time for the period of January 1 – February 28, 2009 (DOY 1 – 59). Quality assurance was similar to the summer analysis. The u* (> 0.2 m s^{-1}) filter removed 19% of the data, and the stationarity filter using CO_2 and CO removed an additional 7% of data.

The observed BTEX concentration patterns (Figure 3.3) exhibited typical trends similar

to those shown for the analysis of summer data (Section 3.1.1). The weekday morning rush hour peaks were followed by a drop and lower daytime abundances, while lower concentrations without a significant rush hour peak were observed during the weekends. The rush hour peaks occurred about an hour later compared to the traffic counts, due to a later breakup of the morning boundary layer. Early morning minima occurred around 4:00 -5:00 h. Daytime BTEX minima generally occurred in the afternoon, again likely a result of reduced emissions into the maximum BL height at that time. Typically, the second rush hour (15:00 – 18:00 LST) peaks were observed earlier (18:00 – 21:00) compared with the summer time results as a result of different BL dynamics in winter.

For representativeness, values calculated from all observed wind directions are shown in Table 3.4 as the results. The concentrations of toluene and xylene were 75% and 60% of those during summer time, respectively, while the concentration of ethylbenzene is similar. The median concentration of benzene was 10% higher than that in summer. Comparing the summer and winter values (Table 3.1 and Table 3.4), the higher benzene concentration in winter time is in agreement with the higher winter concentration values measured at the Houston Aldine site (Smith et al., 2007), located relatively far from the petrochemical industrial sources.

Table 3.4
Winter BTEX mixing ratios (in ppb = nmol mol^{-1}; LDL = lower detection limit).

	Max.	Mean	Median	Min.
Benzene	1.80	0.38 0.65[a]	0.31	0.01
Toluene	2.42	0.43	0.32	<LDL
Ethylbenzene	0.30	0.06	0.05	<LDL
Xylenes	1.32	0.28	0.22	0.04

[a] recalculated value based on the summer/winter ratio and the annual trend at the Aldine site (Reiss, 2006).

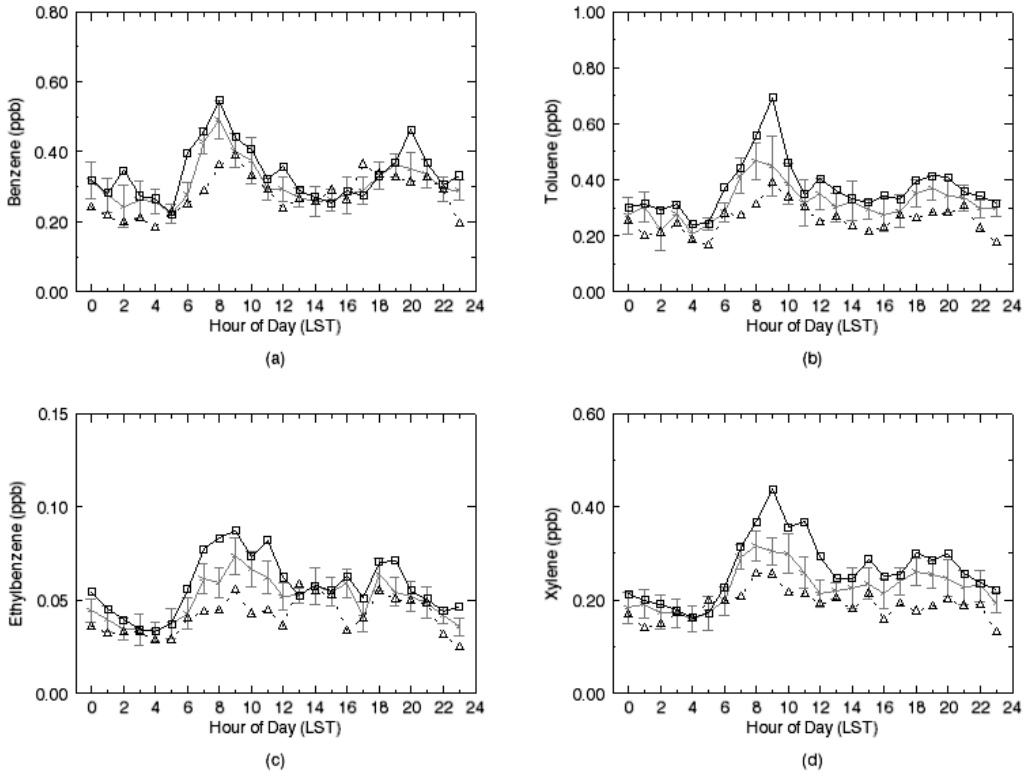

Figure 3.3. Same as Figure 3.1, but for winter time (January + February 2009).

Median diurnal flux variations of the BTEX compounds in wintertime are shown in Figure 3.4, with statistics listed in Table 3.5. Overall, we found mean fluxes of toluene to dominate BTEX flux, followed by xylenes, benzene and ethylbenzene. None of the BTEX compounds showed prominent morning or afternoon traffic rush hour peaks. The dominant morning peaks instead occurred 2-3 hour later.

A weak weekend evening peak (higher than during weekdays) was observed, likely due to increased car traffic (Figure 2.3). During daytime, toluene and xylene also showed dominant peaks, but clear weekday-weekend differences were not observed for all compounds compared with the summer results. This strongly suggests that the contribution of evaporative emissions to the total fluxes – measured during the summer time in this area – was significantly suppressed because of the lower winter temperatures.

Table 3.5
Statistics for the measured fluxes of BTEX (in mg m^{-2} h^{-1}) for all wind directions in winter.

	Benzene	Toluene	Ethylbenzene	Xylenes
Max	1.52	4.54	0.86	4.33
Mean	0.21	0.35	0.07	0.23
Median	0.17	0.24	0.04	0.14
SD	0.23	0.47	0.09	0.35
N	679	706	497	474

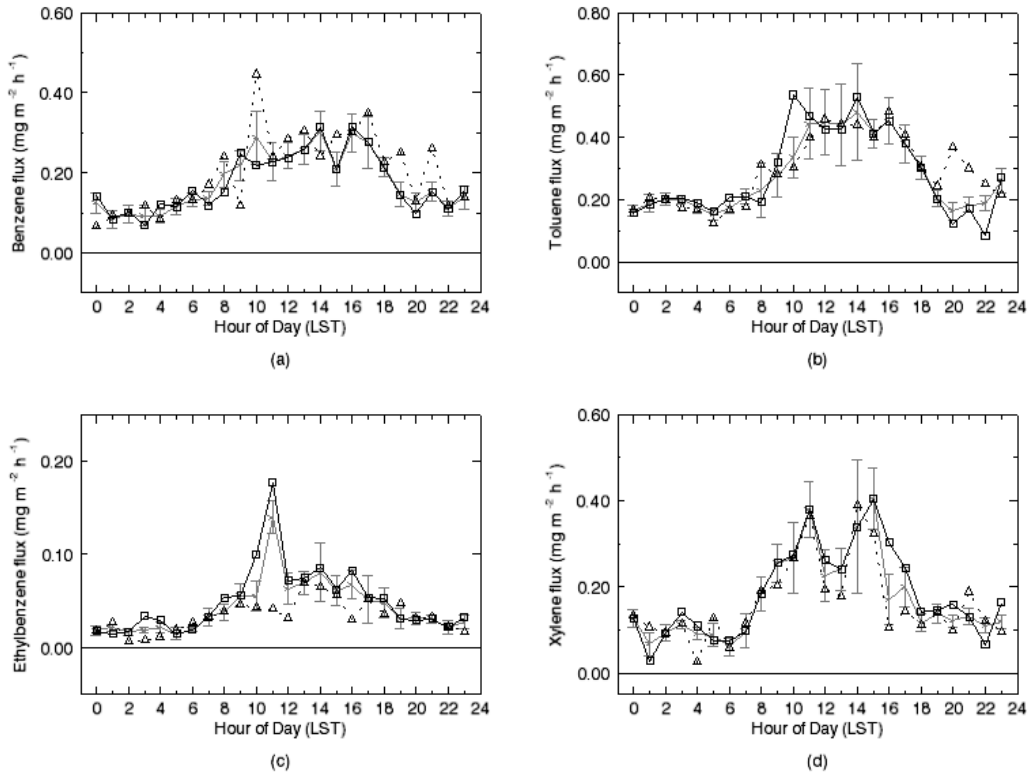

Figure 3.4. Same as Figure 3.2, but for winter time (January + February 2009).

3.3. Discussion

BTEX aromatics are highly volatile, with toluene and xylenes used as solvents in several industries. Our summer data clearly indicate evaporative emissions of these species during weekday working hours. While this could be driven by evaporative emissions from gasoline during higher daytime temperatures, the lack of a maximum evaporative impact during the hottest daytime hours suggests otherwise. We found that the flux ratio of toluene to benzene (T/B ratio) was, on average, higher than 4 during the working hours, while nearly stable around 1.5 during the rest of the day. Compared to work by Gelencser et al. (Gelencser et al., 1997) and Schnitzhofer et al. (Schnitzhofer et al.,

2008), this suggests that heavy duty engine emissions contributed only a small amount of total emissions in our footprints, and that working hour emissions are likely not explained by gasoline evaporation alone. We estimated the fraction of evaporative emissions based on the normalized total BTEX flux, compared with normalized CO_2 fluxes and traffic counts, shown in Figure 3.5. Assuming that CO_2 fluxes are dominated by traffic because photosynthetic uptake during daytime was reduced as the result of the drought, and further assuming that BTEX to CO_2 tailpipe emission ratios are diurnally stable, the difference in flux pattern between traffic and BTEX compounds as a function of daytime can be used to infer the evaporative fraction. As the diurnal variation of the CO_2 flux correlated well with the traffic pattern during the morning hours (Figure 3.5a), and although photosynthetic uptake seems to become more relevant after the noon hours, the assumptions appear reasonable. The evaporative fraction of total BTEX emissions in summer can then be calculated for each hour from the difference between the relative drop in traffic counts and the lack of a drop of BTEX flux throughout the day. Integrated over the whole day, the evaporative flux contribution averaged 34% for total BTEX flux, dominated by toluene and xylenes during summer (Figure 3.5(a)).

The observed weekday working hour enhancements of toluene and xylenes fluxes in summer are likely related to local emissions as a result of solvent use in paint and metal workshops within two hundred meters of the tower, and possibly also gasoline evaporative emissions from the large fleet of cars Yellow Cab handles at this location.

We interpret them as part of the evaporative emissions typically contributing to urban BTEX abundances, not therefore unusual in this urban setting.

The comparison of extrapolated measurement data to the Harris County EPA NEI, summarized in Table 3.6, revealed large differences. Assuming that traffic emissions dominate, the results should agree with the 'onroad' category, or the sum of the 'onroad' and relevant 'nonpoint' categories, i.e. the extra evaporative emissions. Satisfactory agreement was achieved with the 1999 NEI considering that summer evaporative emissions likely overestimate average annual emissions. Although the methodology likely has uncertainty of at least a factor of two, the discrepancies were clearly outside that range for the 2005 NEI, whether including nonpoint sources or not. In summary, if evaporative emissions from a standing car fleet in the area in addition to onroad vehicles and the local solvent use emissions are significantly overestimated as a result of the high summer time temperatures, the comparison could be improved, and 1999 inventory data reasonably reflects actual emissions. Indeed, a preliminary analysis of our wintertime flux measurements revealed a significant reduction in toluene and xylenes fluxes, consistent with the temperature hypothesis. The winter time evaporative flux contribution was only 20% following the same calculation in summer (Figure 3.5(b)).

Table 3.6
EPA NEI data for Harris County, Texas, compared to this study's extrapolation, in metric tons per year.

Compound	Extrapolated values (this study)		2005 NEI		1999 NEI	
	Total [a]	Separated [b]	Nonpoint [c]	Onroad	Nonpoint [c]	Onroad
Benzene	2,007	1,859	14	678	20	1,524
Toluene	5,195	5,640	403	1,668	916	3,986
Ethylbenzene	590	649	22	268	141	626
Xylenes	4,841	5,098	208	984	368	2,331

[a] extrapolated from the total median values from Table 3.2.
[b] extrapolated from the sum of each day/nighttime and weekday/weekend median flux in Table 3.3.
[c] includes only selected categories (e.g. gas stations, metal surface coating procedures, or consumer products)

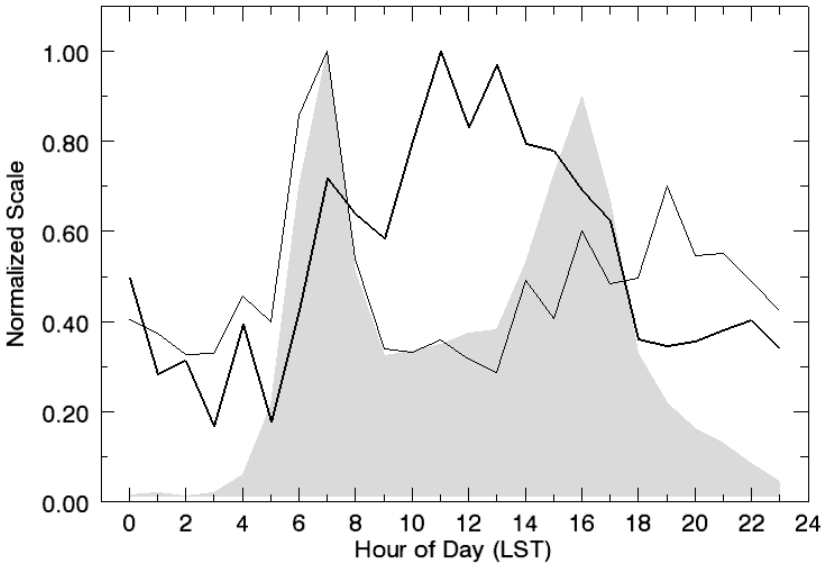

(a)

Figure 3.5. Normalized BTEX flux (thick black line), compared to normalized CO_2 flux (thin black line) and normalized first 30-min vehicle counts (gray shaded area) on the nearby commuter roads (sum of counts shown in Figure. 2.3) in summer (a) and in winter. Relative amounts of evaporative emissions were estimated from the white area between the BTEX and traffic flux curves relative to total area under the BTEX flux curve.

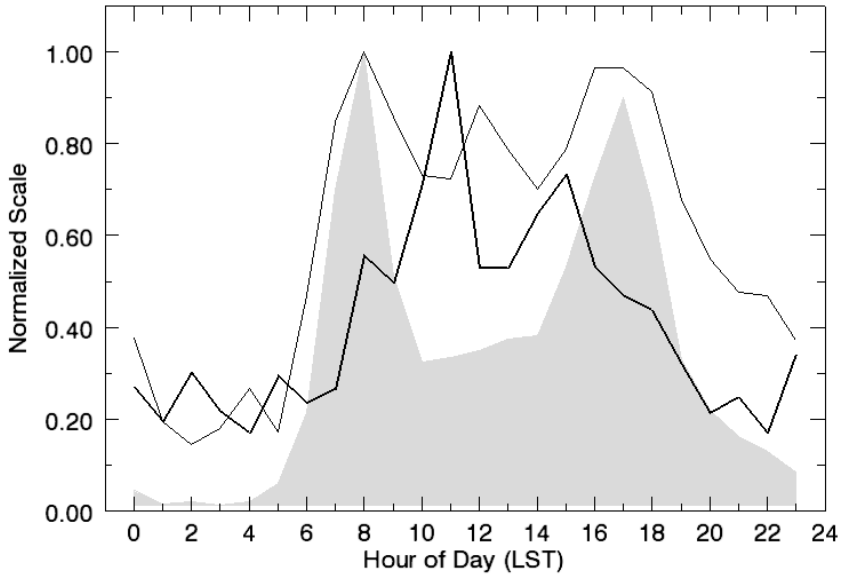

(b)

Figure 3.5 Continued.

To investigate the lack of rush hour peaking observed for the winter data, a footprint analysis (Figure 3.6) and a wind direction analysis (Figure 3.7) were performed. Considering only the southern sector in the summer time analysis, the summer footprints and wind direction were very similar between the morning and the afternoon rush hours for the weekdays, and relatively clear morning and afternoon rush hour peaks were observed (Figure 3.2). However, during winter, using all wind directions, the footprints were significantly different: flux contributions from the commuter roads in the east were lower, and shorter sections of the roads were covered during both rush hours than in the summer. In addition, the wind direction in Figure 3.7 showed also higher variability in

winter and the rush hour fluxes were also significantly lower than the values in summer. This result revealed one possible reason why no obvious morning and after noon peaks in the traffic rush hours were observed during the winter study period.

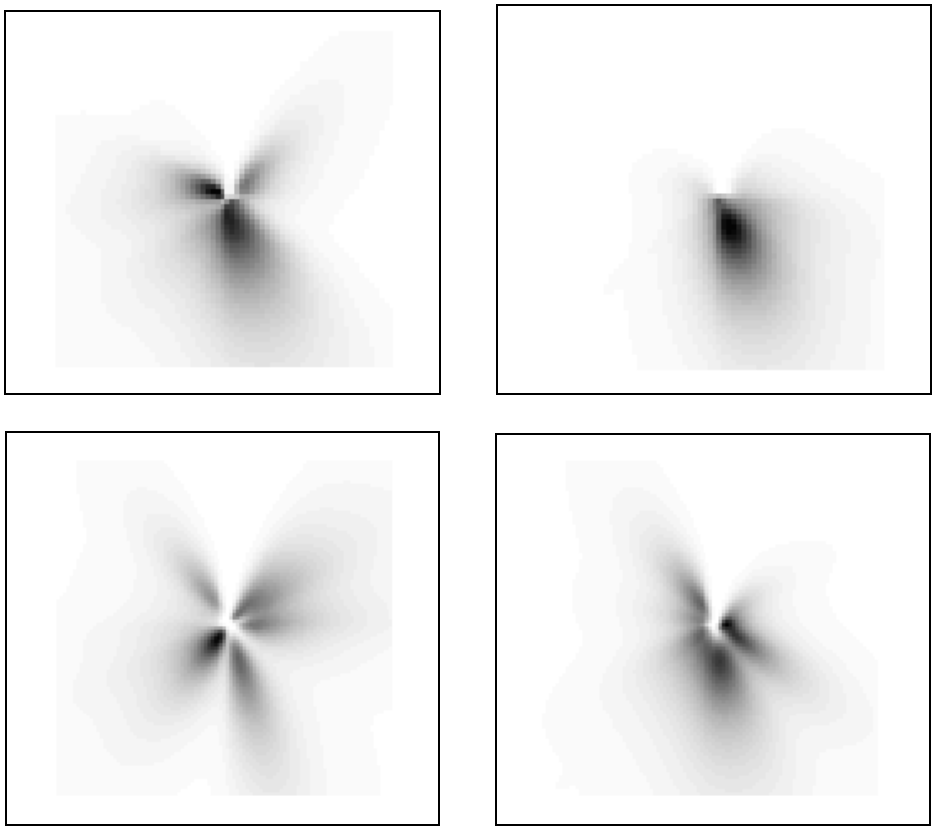

Figure 3.6. Accumulated weekday footprint density (whole period) from Kormann and Meixner's model for the morning rush hour (left panels) and the afternoon rush hour (right panels) in summer (upper panel) and winter (bottom panel) within the 2 km x 2 km study domain. Based on the traffic counts (Figure 2.3), the morning rush hour was 5:00- 8:00 and 6:00 – 9:00, and the afternoon rush hour was 14:00 – 17:00 and 15:00 – 18:00 in summer and winter, respectively, due to daylight saving time in summer. Probability of contribution to an individual flux measurement from a single 30x30 m^2 pixel increases from white to black shading.

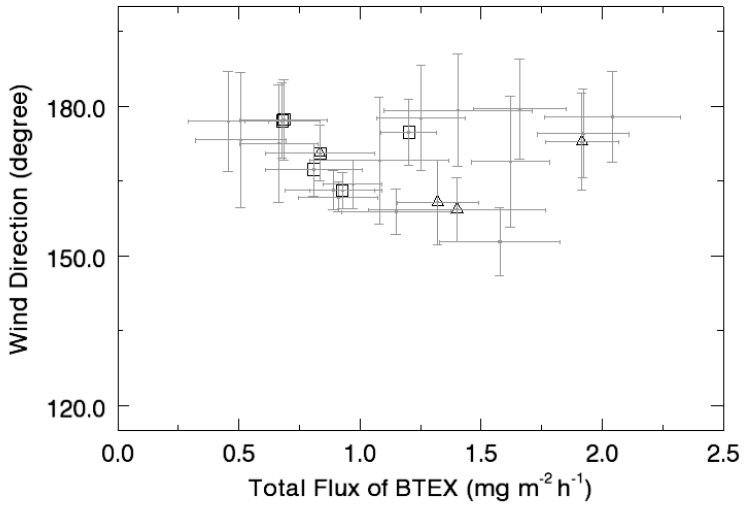

(a)

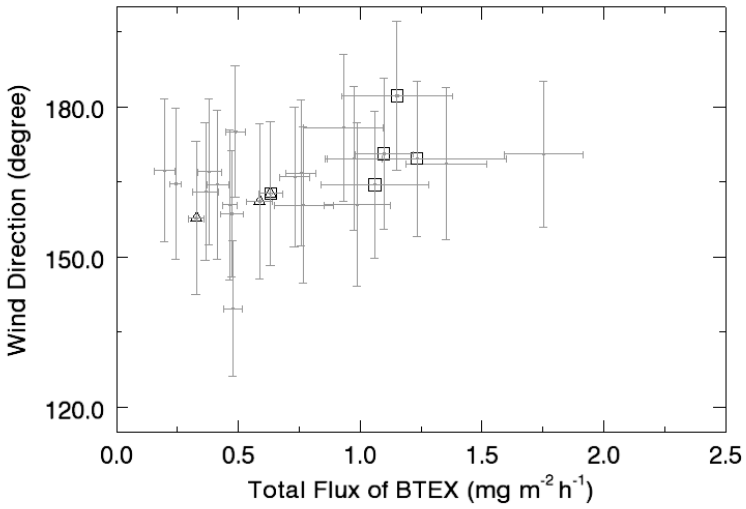

(b)

Figure 3.7. Total hourly BTEX flux versus wind direction during summer (a) for southerly wind direction and during winter (b) for all wind directions. Gray dots indicate individual hourly data points with the standard error bars, black triangles indicate the morning rush hours, and black squares the afternoon rush hours.

4. RESULTS OF MIXING RATIO AND FLUX OF ISOPRENE AND ITS OXIDATION PRODUCTS

4.1. Isoprene

We present the results of measured mixing ratios and fluxes of isoprene and its oxidation products for the same summer period and analyzed the same way as for the BTEX species (Section 3.1). We analyzed the data temporally separated between the hours 6:00 – 9:00 LST, "rush hour" and "daytime" hours 10:00- 18:00 LST to evaluate both biogenic and anthropogenic emission sources and investigate emission characteristics.

4.1.1. Isoprene concentration

Figure 4.1 shows the median diurnal variation of isoprene mixing ratios in updrafts. As expected for a biogenic emission such as isoprene, minimum abundances were generally measured around sunrise. Maxima appeared during daytime (13:00- 16:00) likely as a result of light and temperature driven biogenic emissions. Although daytime abundances were generally much lower compared to forested regions (Biesenthal et al., 1997; Helmig et al., 1998; Montzka et al., 1993) nighttime mixing ratios appeared to be much higher than in rural environments (~20 ppt (Apel et al., 2002)), which indicates either an unidentified NMHC underlying the chromatographic peak of isoprene or a low-level, non-biogenic isoprene emission at night. The rush hour peak (06:00 – 09:00) was expected based on previous studies that identified significant tail-pipe emissions of isoprene (Borbon et al., 2001; Derwent et al., 1995; Reimann et al., 2000). Although the

morning peak was a significant feature of weekday versus weekend data, it did not overlap in hour with peaks for the typical tail pipe species benzene and toluene (Section 3.1). While benzene and toluene maximized at 5:00-7:00 after which emissions drop, combined anthropogenic and biogenic isoprene emissions maximized its abundance slightly later. Similar to previous studies, there was no clear signature of tailpipe emissions during the evening rush hour because emissions occur into a much deeper afternoon boundary layer.

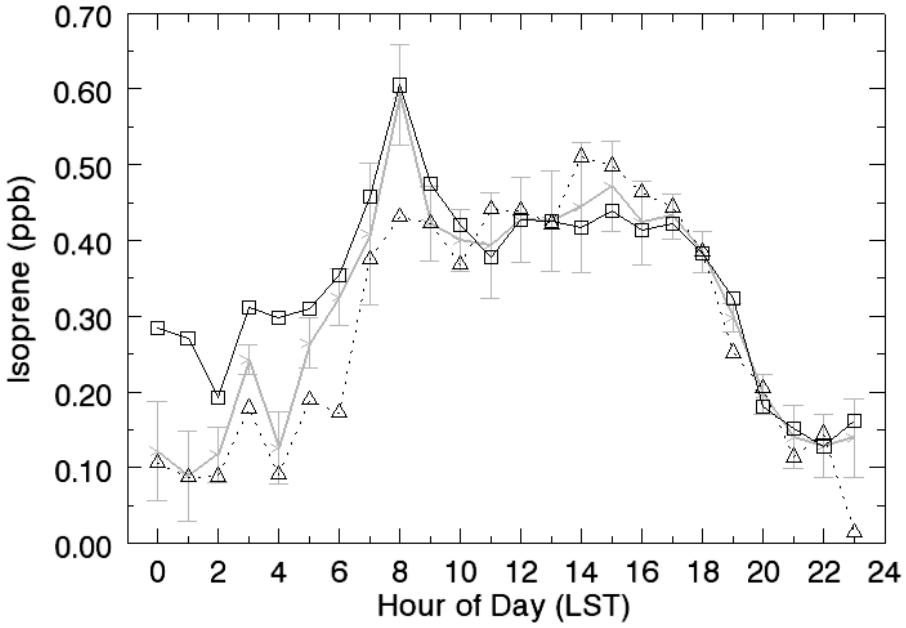

Figure 4.1. Diurnal median variation of the mixing ratio of isoprene during the study period. The thick grey line with error bars (standard error) shows medians; the square-solid and the triangle-dotted lines show weekday and weekend, respectively.

In Table 4.1, the observed concentrations of isoprene are compared with results of previous studies in Houston. Our mean value is lower compared to sites with higher near-by tree densities but larger compared to sites closer to the Houston Ship Channel (La Porte, Clinton). Isoprene abundance at other urban sites, such as 0.36 ppb in Central London (Derwent et al., 1995), or 0.29 ppb in Lille, France (Borbon et al., 2001), were comparable to our mean, while higher values up to 1.0 ppb were (only anthropogenic) measured in urban Mexico City, Mexico (Fortner et al., 2009), interpreted as being of anthropogenic origin.

Table 4.1. Isoprene mixing ratios in Houston (in ppb = nmol mol^{-1}; LDL = lower detection limit).

	Max.	Mean	Median	SD
This study				
Rush hour	1.78	0.63	0.48	0.46
Daytime	1.50	0.46	0.42	0.21
Deer Park [a]		0.83		
Bayland Park [a]		0.67		
Williams tower [b]		0.58		
La Porte	26.5 (28.8) [c]	0.3 (0.3) [c]	0.11-0.182 [f]	
		0.48 [d], <0.1 [e]		
Clinton		0.17 [d]		

[a] measured by PTR-MS in September 5-27, 2006 and reported by Houston Advanced Research Center (http://files.harc.edu/Projects/AirQuality/Projects/H075/H075ExecutiveSummary.pdf)

[b] recalculated value based on the reactivity (Berkowitz et al., 2005) and the OH reaction rate constant during TexAQS 2000 (Atkinson, 1994).

[c] measured by PTR-MS and GC-FID (in parenthesis) during TexAQS 2000 (Karl et al., 2003)

[d] averaged value measured at 6 m height during TexAQS 2000 (Song et al., 2008).

[e] measured by PTR-MS at 10 m height during TexAQS 2000 (Kuster et al., 2004).

[f] observed range of three different type of measurements during TexAQS 2000 (Jobson et al., 2004).

4.1.2. Isoprene flux

Figure 4.2 depicts the median diurnal variation of isoprene fluxes. Mean and median daytime fluxes were 0.56 mg m^{-2} h^{-1} and 0.49 mg m^{-2} h^{-1} respectively. The flux pattern showed a peak during the morning rush hour and a second peak in the afternoon (12:00-14:00 LST) as expected from a biogenic source. Interestingly, somewhat higher weekend than weekday afternoon fluxes were observed. The daytime flux during weekend is up to 20% higher than that in weekdays, which is discussed later in section 4.3.

Due to a lack of isoprene flux data in urban areas and Texas in general, we only compared with previous studies at rural or forested sites including a boreal aspen forest in Canada (1.2 mg m^{-2} h^{-1}; (Baldocchi et al., 1999), western Alabama and eastern Georgia (12.5 mg m^{-2} h^{-1} and 5.4 mg m^{-2} h^{-1},respectively; (Guenther et al., 1996), and the AmeriFlux site of the University of Michigan Biological Station (2.8 – 3.2 mg m^{-2} h^{-1}(Apel et al., 2002; Pressley et al., 2005). These showed that our flux values were lower by a factor of 2 to 10. As expected, values were significantly lower than these previous studies in rural and forest sites, considering the low density of isoprene emitters.

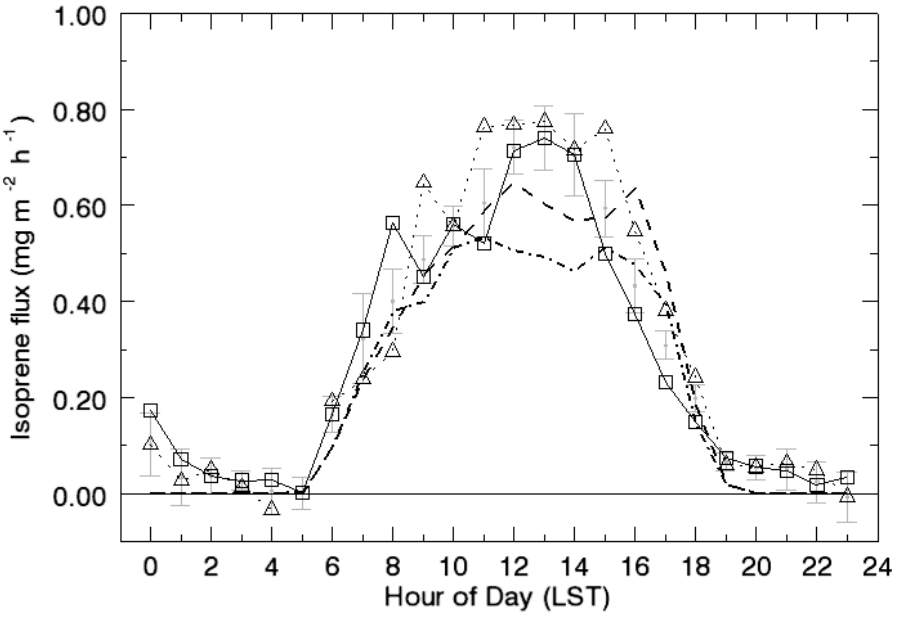

Figure 4.2. Same as Figure 4.1, but for isoprene flux. Black dashed line indicates the result of Guenther's model for weekdays, dashed-dotted line indicates the model's results for weekends.

The emission rate of isoprene from plants is dominantly influenced by incident light and leaf temperatures. Figure 4.3 shows the observed relationships of measured isoprene fluxes with PAR and ambient temperatures during daytime alongside isoprene emission model estimations using the standard T&PAR parameterization (Guenther et al., 1995; Guenther et al., 1993). To avoid the effect of rush hour emissions, only data from 10:00 – 18:00 h were used. Leaf temperatures were assumed to be equal to air temperature measured at the lowest tower level (14.2 m agl, close to average tree leaf level) on the flux tower. Using an average basal emission rate of 0.53 mg m^{-2} h^{-1} under the condition

of $\overline{T} < 30 \pm 2°C$ and PAR > 1000 μmol m^{-2} s^{-1}, we find excellent agreement between modeled and measured average values. Although there appears to be a slight underestimation of the PAR and temperature response by the model, the evaluated ranges were too narrow and the confidence in the flux measurements not high enough to conclude that the discrepancy is significant.

In urban areas a complication is added to the emission and chemistry of isoprene because it is also emitted from anthropogenic sources, in particular as a tail-pipe emission (Borbon et al., 2001; Derwent et al., 1995; Reimann et al., 2000). Although anthropogenic isoprene emissions are considered small compared to biogenic emissions and the density of isoprene emitting trees in urban areas is generally much lower than in forested areas, it may still be a major source of ozone formation (Chameides et al., 1988; Geron et al., 1995). A recent study of NMHC in US cities demonstrated that isoprene is the most dominant unsaturated NMHC in nearly half of the cities (Baker et al., 2008). To estimate the amount of potential anthropogenic isoprene emissions, we subtracted the modeled isoprene flux from our measured isoprene flux for the weekday rush hour (5:00 – 8:00 h) period. The result showed a potential (tail-pipe) emission of anthropogenic isoprene was up to about 30% of the total measured isoprene flux during the weekday morning rush hour (Figure 4.2).

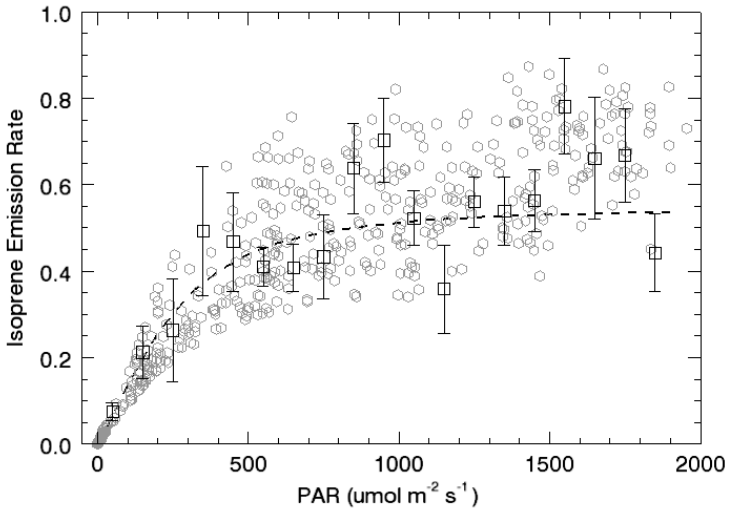

(a)

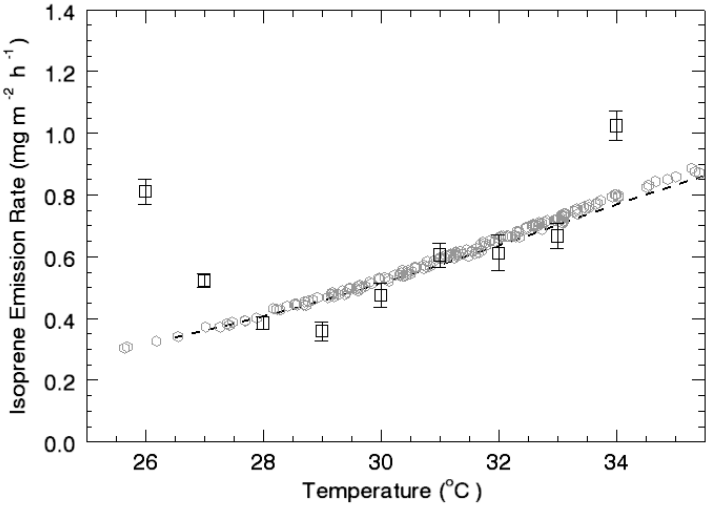

(b)

Figure 4.3. (a) Relationship between isoprene flux and PAR values during daytime, and (b) relationship between isoprene flux and air temperature. Dashed line represents the T&PAR model (Guenther et al. 1993). Open squares are measured median values for 100 PAR unit intervals, respectively 1˚ intervals, error bars are respective standard errors, and gray circles are the model results with the measured temperature and PAR input values. The presenting condition is: air temperatures of 30 ± 4°C and PAR > 1000 µmol m^{-2} s^{-1} with the estimated basal emission rate of 0.53 mg m^{-2} h^{-1}.

4.2. Isoprene oxidation products

MACR and MVK are the major oxidation products of the OH initiated oxidation of isoprene during daytime, and probably also during nighttime as initiated by ozone and nitrate radicals. The MVK/MACR ratio typically increases with time of day and the relative production rate of MVK to MACR from isoprene (e.g. (Montzka et al., 1993; Stroud et al., 2001)) is ~1.4, because of the longer life time of MVK than MACR towards OH radical reaction. In addition to the isoprene oxidation products, MACR and MVK are also known as direct vehicular emissions: Jonsson et al. (Jonsson et al., 1985) suggested the direct vehicular emission of these compounds by comparison with simultaneous aromatic VOCs measurements in Los Angeles, California, while Biesenthal and coworkers (Biesenthal and Shepson, 1997; Biesenthal et al., 1997) showed a high correlation of MACR and MVK with CO in Toronto, Ontario, Canada, during winter. Direct MACR emissions were also inferred from onroad measurements (Grosjean et al., 2001; Kean et al., 2001).

Table 4.2. Mixing ratio of isoprene oxidation products measured in this study and previous studies in rural/forest area in summer (in ppb = nmol mol^{-1}; LDL = lower detection limit).

	MACR			MVK		
	Max.	Mean	Median	Max.	Mean	Median
This study (daytime only)	0.38	0.13	0.12	0.42	0.13	0.12
Montzka et al. (1993)		0.66			0.98	
Trainer et al. (1987)		0.60			0.75	
Biesenthal et al. (1997)		0.30			0.75	
Stroud et al. (2001)		0.2			0.36	
Spaulding et al. (2003)		0.34±0.15			0.51±0.29	
	MACR + MVK in Houston [a]					
Deer Park	0.55±0.12					
Bayland Park	1.26±0.85					

[a] measured by PTR-MS in September 5-27, 2006 and reported by Houston Advanced Research Center (http://files.harc.edu/Projects/AirQuality/Projects/H075/H075ExecutiveSummary.pdf)

Here, we discuss MACR and MVK concentrations and fluxes as related to the isoprene fluxes shown above, and its chemistry. Figure 4.4 shows the observed mixing ratio and flux diurnal patterns of MACR and MVK, with statistics given in Table 4.2. Abundances were relatively low as compared to environments with higher isoprene emitter density (Biesenthal et al., 1997; Montzka et al., 1993; Spaulding et al., 2003; Stroud et al., 2001; Trainer et al., 1987). As the uncertainties of the calculated fluxes increase rapidly with decreasing concentration, only mixing ratios above 20 ppt were considered in the REA flux calculation. Interestingly, the oxidation products displayed significantly different diurnal patterns: While MACR showed higher nighttime mixing ratios especially between weekdays and weekends, MVK mixing ratios were apparently much more similar to isoprene. While MACR fluxes displayed a morning rush-hour peak, MVK did

not. These observations are consistent with the notion that MACR is emitted anthropogenically (Biesenthal and Shepson, 1997; Grosjean et al., 2001; Kean et al., 2001), mostly likely in tailpipe exhaust.

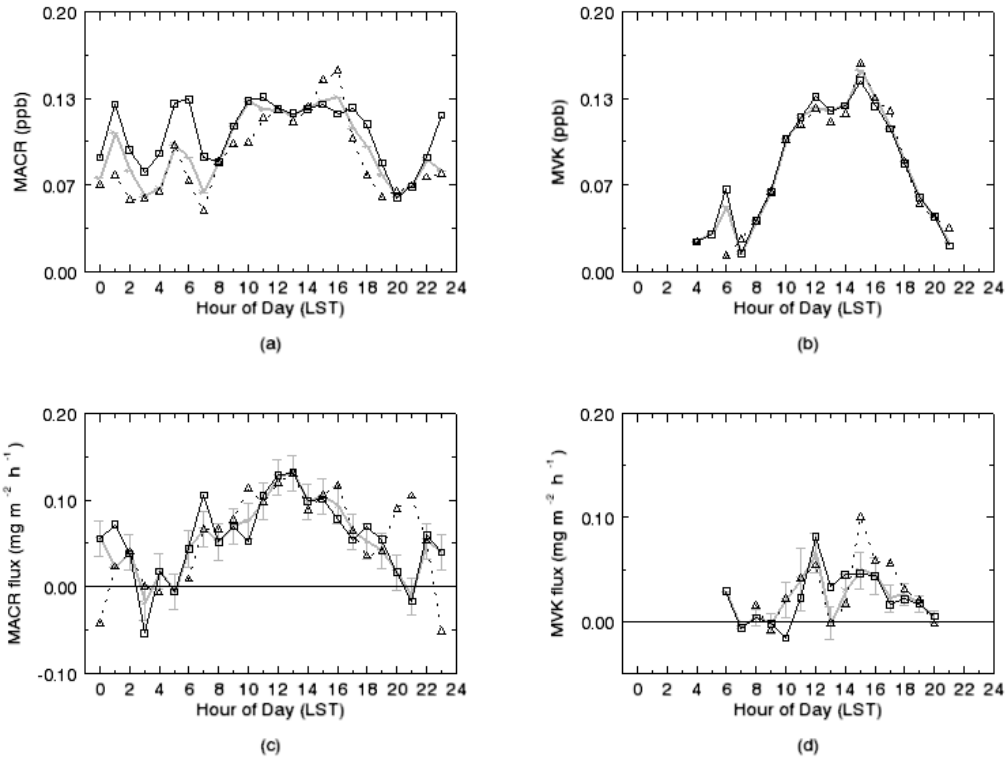

Figure 4.4. Diurnal median variation of mixing ratio in updrafts of MACR and MVK during the study period. The thick grey line with error bars (standard error) shows the medians; the square-solid and the triangle-dotted lines show weekday and weekend trends, respectively.

Nevertheless, isoprene explained the dominant amount of variability in MACR and MVK mixing ratios. It is likely the dominant source of these species in this part of Houston. Several previous studies have compared isoprene oxidation product

abundances with its precursor to illuminate in-situ isoprene chemistry (Apel et al., 2002; Stroud et al., 2001). We reproduced some of these analyses here. Considering the background concentration of MACR ~40 ppt (Figure 4.5), our daytime concentration ratio of MVK to MACR was ~1.4 suggesting a photochemically very young source. The additional anthropogenic MACR source is corroborated by the ratio of ~0.45 during the morning rush hour (Figure 4.5 triangles), indicative of MACR not dominantly supplied by isoprene oxidation.

The ratios of MACR/isoprene and MVK/isoprene contain useful information on the photochemical age of measured isoprene in an air mass, introduced by Stroud et al. (Stroud et al., 2001) and Apel et al. (Apel et al., 2002). We derived an expression for the time rate of change in the MACR/isoprene and MVK/isoprene ratios – adopting the analysis of Stroud et al. (Stroud et al., 2001) – as a function of [OH], the rate coefficients and the time available for processing, and investigated the relationship measured. A sequential OH-driven isoprene oxidation mechanism under NOx-rich conditions proceeds as follows (Carter and Atkinson, 1996) :

$$\text{Isoprene} + \text{OH} \xrightarrow{k1} a\,\text{MACR} + b\,\text{MVK} \qquad (4.1)$$

$$\text{MACR} + \text{OH} \xrightarrow{k2} \text{products} \qquad (4.2)$$

$$\text{MVK} + \text{OH} \xrightarrow{k3} \text{products} \qquad (4.3)$$

Solving this consecutive reaction scheme under the assumption of a pseudo-first-order reaction (OH constant), the result is:

$$[MACR]/[Isoprene]=[a\,k_1\,(1-\exp(k_1-k_2)[OH]_{avg}{}^{t})]/(k_2-k_1) \quad (4.4)$$

$$[MVK]/[Isoprene]=[b\,k_1\,(1-\exp(k_1-k_3)[OH]_{avg}{}^{t})]/(k_3-k_1) \quad (4.5)$$

where a = 0.23, b = 0.32, k_1= 1.0 x 10^{-10} cm^3 $molecules^{-1}$ s^{-1}, k_2 = 3.3 x 10^{-11} cm^3 $molecules^{-1}$ s^{-1}, and k_3 = 1.9 x 10^{-11} cm^3 $molecules^{-1}$ s^{-1}.

The expression is purely chemical and does not include any mixing processes which may affect the ratio during transport. Here our purpose of the investigation of the relationship with isoprene and its oxidation products is to reveal the anthropogenic emission sources of MACR besides isoprene oxidation.

Figure 4.6 shows a mostly well-defined relationship of MACR and MVK with isoprene. The direct isoprene oxidation products MACR and MVK measured at this site were obviously produced within about 0.3 hours for typical OH concentrations between 1 to 2 x 10^7 cm^3 $molecules^{-1}$ s^{-1} (Olaguer et al., 2009) during the TexaQS II study.
In comparison with the studies in forest sites (Apel et al., 2002; Stroud et al., 2001) and our midday values, data during the morning rush hour fell under the theoretically calculated line, shifted toward the x-axis.

This can be explained by a continuous (anthropogenic) MACR emission during the entire day leading to the background MACR mixing ratio of approximately 40 ppt.

During the rush hour, this manifests inself in an even stronger contribution to ambient mixing ratios, which also suggests that there are significant, direct MACR sources besides isoprene oxidation, likely taipipe exhaust emissions.

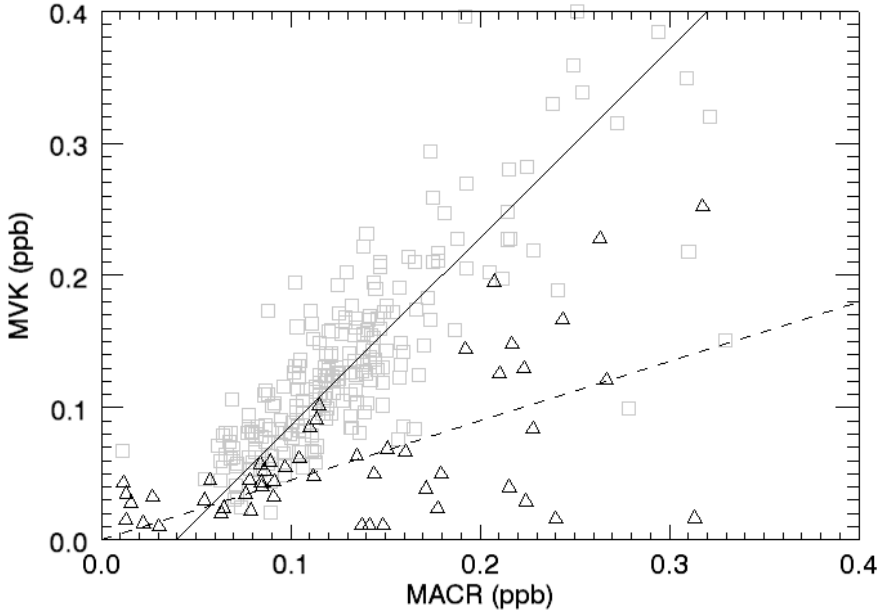

Figure 4.5. Scatter plot of concentration of MACR versus MVK for weekdays. Grey squares are daytime data and black triangles in the morning rush hour period. Black line indicates the slope of 1.4 with 40 ppt MACR background and dashed line 0.45.

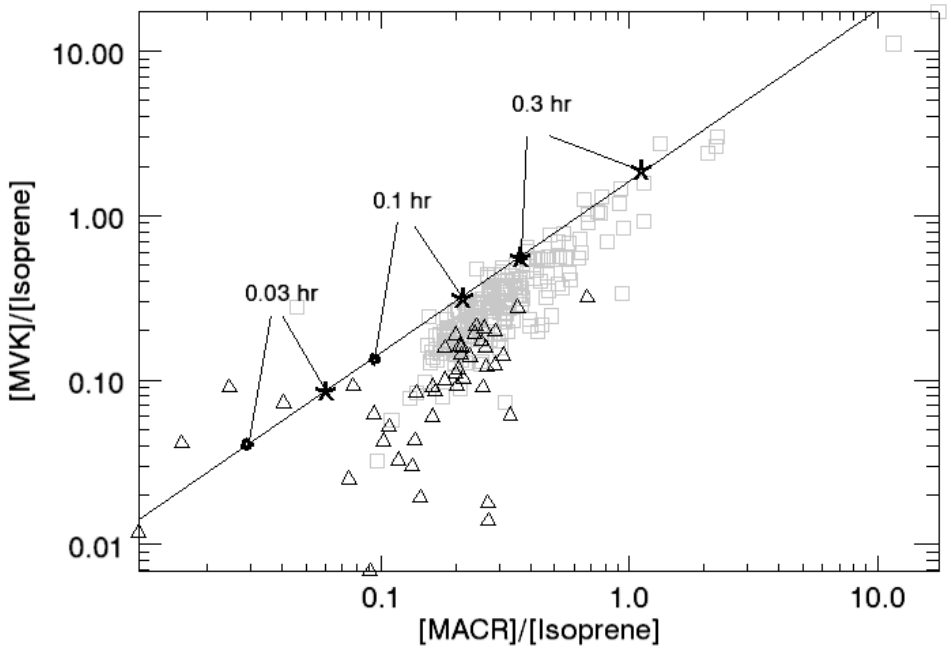

Figure 4.6. Scatter plot of the ratio of MACR/isoprene versus MVK/isoprene. Gray squares are daytime data and black triangles in rush hour period. Black line is the model result of MACR production rate of isoprene oxidation by OH. Circles and asterisks indicate the time makers of the theoretical isoprene oxidation process when [OH] = 1 and 2 x 10^7 molecules cm^{-3}, respectively.

4.3. Discussion

Our daytime measured mixing ratio and flux of isoprene showed a good agreement with previous studies, and also showed the potential for anthropogenic emission sources of isoprene and MACR, most obvious in the morning rush hour data. To investigate the higher isoprene flux during weekend daytime as well as to trace the origin of the anthropogenic sources, we used footprint climatology analysis.

For the footprint analysis, we calculated the flux footprint (FFP) area by using EdiRe flux analysis software (see section 2.5.3). We first converted all footprint grids into binary grids (1 == cell contributed to flux; 0 == cell did not contribute to flux) and accumulated them (level 1), which provides a density map of areas that contributed to the average flux measured at the tower. We also accumulated all footprint density grids (level 2). Next, we multiplied each grid with the measured isoprene flux and again accumulated them (level 3), which provided a weighted flux density grid. Lastly, to avoid directional biases as a result of the inhomogeneous wind direction distribution during our study, we divided the level 3 grid by the level 1 grid to arrive at a normalized weighted flux density grid (level 4):

$$\text{Normalized Weighted FFP} = \frac{\sum_{\text{hour}} \{(\text{Isoprene Flux}) \times \text{FP}\}}{\sum_{\text{hour}} \{\text{Count of FP in Each Grid}\}} \qquad (4.6)$$

Figure 4.7 shows this footprint analysis for rush hour and daytime, respectively, within the study domain shown in Figure 2.1. The actual FFP (level2) was covering dominantly areas maximally 1 km from the tower towards the SE, except during rush hour periods. During daytime, the normalized weighted FFPs covered the relatively tree dominant southern area when the number of vehicles was lower and the biogenic isoprene emission was highly active. On the other hand, during the morning rush hour the normalized weighted FFPs covered also the NE part of main commuter roads and southern sector, at a time before the isoprene photooxidation matters. Higher emissions from the NW side of the tower, though that wind direction was rarely encountered, are

consistent with our finding of a higher oak tree density 100-300 m from the tower. Lower emissions from the east as compared to the SE and S are consistent with a generally higher tree density in southern directions as compared to eastern directions (note that northerly winds were very rarely encountered during the study period; Figure 2.2). Significant flux contributions from the NE during rush hour are consistent with the fact that only 100-200 m east of the tower run the two one-way, three-lane commuter roads (Hardy/Elysian Streets in Figure 2.1), which maximally overlap the FFP under SE and NE wind directions. Most rush-hour traffic in the FFP domain occurs on these roads. This different FFP spatial distribution again shows that there were obviously significant isoprene emissions during rush hour.

Comparing the footprints between rush hour (Figure 4.7 upper panel)) and daytime (Figure 4.7 middle panel) during weekdays, the potential anthropogenic isoprene flux of 30 % during rush hour was from the main commuter roads before the biogenic emission was very active. During daytime, the footprint also covered these roads, but the amount of biogenic emission was now significantly higher than anthropogenic emission.

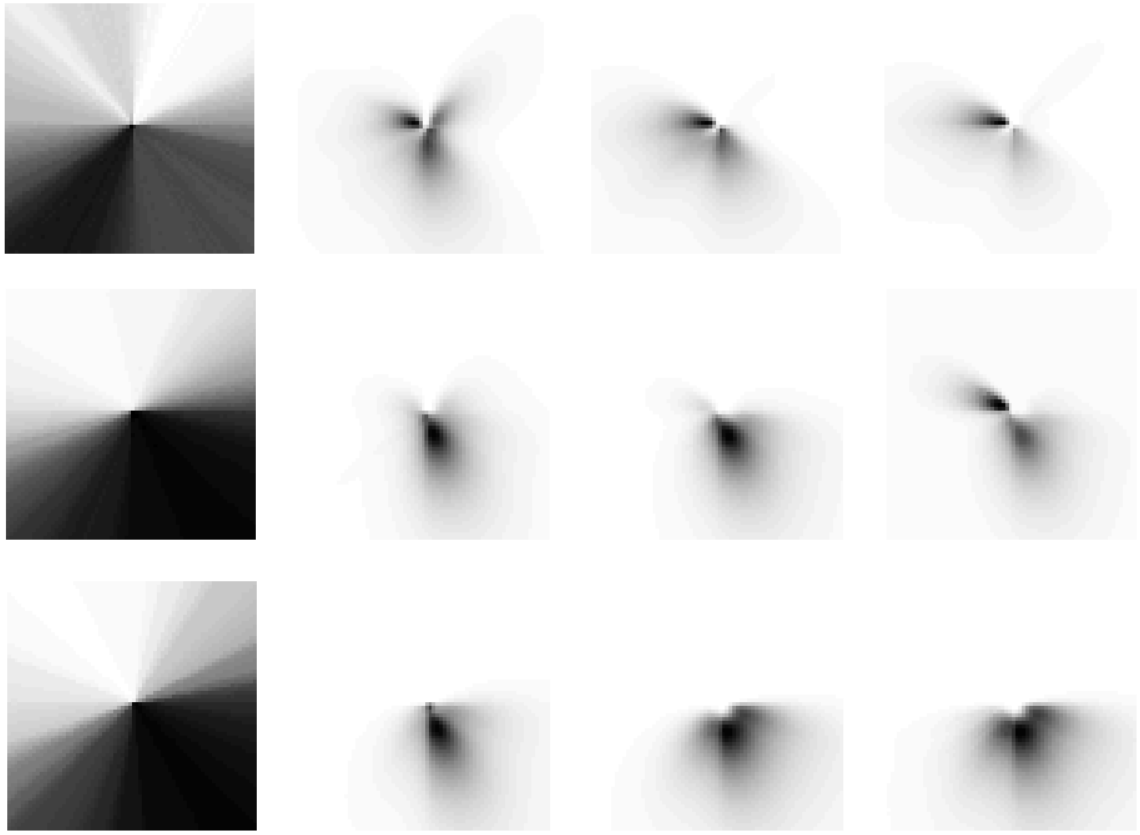

(a) (b) (c) (d)

Figure 4.7. Flux footprints of 2 km x 2 km domain centered by the flux tower, during rush hour (upper panel), during daytime (middle panel) on weekdays, and during daytime on weekends (bottom panel). (a), (b), (c) and (d) indicate the level 1 FFP, level2, level 3 and level 4, respectively, in the text. Probability of flux contribution increases from white to black shading.

As we have reviewed in the previous section 4.1, the daytime isoprene flux on weekends was somewhat higher than that on weekdays. Interestingly, PAR, leaf level temperature and wind speed were all lower on weekends, and there was no obvious difference in the diurnal variation of NOx between weekdays and weekends. Therefore, we investigated the footprint to resolve this conflict (Figure 4.6). During weekend daytime, the footprint was wider and its probability is more intensive in the south than that during weekday

daytime (Figure 4.6. middle panel), which revealed that the higher isoprene emission during weekend daytime was mainly due to the footprint difference. All southern direction footprint overlap significant canopy contribution areas.

MACR and MVK fluxes were low and variable. The median and mean values of the flux of MACR were described in Table 4.3. As MVK fluxes are typically less than 10% of isoprene fluxes, we hypothesized that MVK fluxes could be due to isoprene oxidation between its time of emission in the footprint and air entry into our sample line, while MACR flux could be a combination of anthropogenic emissions and isoprene oxidation. Using the online flux footprint tool of N. Kljun (http://footprint.kljun.net), we calculated crosswind integrated footprint sizes for typical unstable conditions during the measurement period. We then calculated a distance-weighted isoprene transport time between emission and sampling points using average horizontal wind speeds. As OH radical mixing ratios in Houston have been observed to be very high, typically between 1 and 2×10^7 molecules cm^{-3} (Olaguer et al., 2009), the isoprene lifetime can be less than 20 minutes (Figure 4.6). As our calculated transport times are also on the order of minutes, isoprene loss becomes a significant source of its oxidation product flux.

In “reverse”, if we estimate the OH molecular density needed to sustain a MVK flux as shown in Figure 4.4(d), we find that [OH] is low in the morning hours ($< 5\times10^6$ molecules cm^{-3}), rapidly increases after 9 am to maximize at ~3×10^7 molecules cm^{-3} around noontime, then is maintained at high values (1-2×10^7 molecules cm^{-3}) until

sunset. This is in good agreement with the data presented by Olaguer et al. (2009) except for the high late afternoon OH levels. Although the latter maybe maintained by very high ozone and peroxy-radical levels under increasing NO during the late afternoon hours, this was not observed during the TexAQS II (Olaguer et al., 2009). The small MVK fluxes after 18:00 h, when [OH] is expected to drop to very low levels, may therefore either indicate an isoprene emission independent source, such as car traffic, or simply measurement uncertainty as those fluxes are insignificantly different from zero.

In Table 4.4, we summarize our results of this calculation. Using an MVK yield of 32%, we estimate a potential MVK flux range of 0.03 to 0.08 mg m^{-2} h^{-1}. This range encompasses many of the measured MVK fluxes and therefore supports our hypothesis. The MVK, similarly MACR, fluxes could be dominated by isoprene oxidation below the 60-m inlet height. In turn, this means that canopy level isoprene fluxes were likely 7%, up to 29% higher than measured at the 60-m tower level.

Table 4.3. Flux of MACR and MVK in mg m^{-2} h^{-1}.

	MACR		MVK	
	Mean	Median	Mean	Median
Rush hour (weekday)	0.10	0.09	0.03	0.03
Daytime				
(weekday)	0.08	0.07	0.02	0.01
(weekend)	0.07	0.07	0.00	0.02

As shown above, we find good agreement between measured average flux values and modeled flux values. The determined basal emission rate can be compared to the rate

expected from the identified isoprene emitters in the footprint areas of the tower, namely live oak, post oak, water oak, and willow oak. Using an average canopy coverage of 26% (Source: USGS National Map Seamless Server, http://seamless.usgs.gov) in the south of the tower, which far dominated source areas during our measurements, an oak contribution to that cover of 19±8% (in southern sector only), and a specific leaf area of 100±20 $cm^2 g^{-1}$, we estimate a leaf-based basal emission rate of 60 - 99 μg C $g^{-1} h^{-1}$, which is in agreement with a species-weighted average of 46 – 81 μg $Cg^{-1} h^{-1}$ using data from (Geron et al., 2001) under the assumption that leaf area index (LAI) of sunlit leaves is roughly 1.0 for all trees. Thus, our measurements may serve as a confirmation that emission models for urban areas that are based on species distribution and leaf area density information provide consistent estimates of biogenic isoprene emissions even in heterogeneous source areas.

Table 4.4. Calculated potential MVK flux depending on the wind speed and [OH] based on a simple parameterization for flux footprint prediction.

Wind Speed (m)	3	4	5	6
	Under condition of [OH] = 1×10^7 molecules cm^{-3}			
Percent Loss	16%	12 %	10 %	9 %
Potential MVK flux (mg $m^{-2} h^{-1}$)	0.03	0.02	0.02	0.02
	Under condition of [OH] = 2×10^7 molecules cm^{-3}			
Percent Loss	27%	22 %	18 %	16 %
Potential MVK flux (mg $m^{-2} h^{-1}$)	0.05	0.04	0.04	0.03

The calculation was under condition of $\sigma_w = 0.9$, $u^* = 0.6$ ms^{-1}, $z_0 = 1$ ms^{-1}, $z_m = 52$ m, $k_{OH} = 1\times10^{-10}$ cm^2 $molecules^{-1}$ s^{-1}, and the median value of isoprene flux measured.

5. SUMMARY

Despite of the importance of a detailed understanding of VOC fluxes in urban areas for their direct (toxicity) and indirect (local and regional ozone formation) effects on the public health, direct measurements of flux have rarely been executed due to the physically complicated urban structure, a complicated mix of various sources and a lack of suitably accessible measurement platforms. In order to long-term monitor the concentration and the flux of EPA criteria and hazardous air pollutants in urban areas, we deployed tall tower flux equipment onto a private lattice tower in Houston, Texas, and combined it with an REA + GC-FID method for VOCs.

The meteorological and geographical features of our site and the performance of our system were introduced. The diurnal variations of concentration and fluxes of traffic tracers were presented with the selected BTEX measurement results during summer (May 22 – July 22, 2008) and winter (January 1 – February 28), and the measured values exhibited diurnal cycles with a dominant morning peak during weekdays related to rush-hour traffic. The mean and median concentration was 0.51 ppb and 0.36 ppb for benzene; 0.72 ppb and 0.54 ppb for toluene; 0.11 ppb and 0.08 for ethylbenzene; and 0.61 ppb and 0.45 ppb for xylenes, respectively in southern wind direction in summer. The BTEX fluxes also showed rush hour peaks during weekdays, and additional workday daytime flux maxima for toluene and xylenes. The mean and median fluxes were 0.17 mg m^{-2} h^{-1} and 0.17 mg m^{-2} h^{-1} for benzene; 0.58 mg m^{-2} h^{-1} and 0.44 mg m^{-2} h^{-1} for toluene; 0.07 mg m^{-2} h^{-1} and 0.05 mg m^{-2} h^{-1} for ethylbenzene; 0.56 mg m^{-2} h^{-1} and

0.41 mg m^{-2} h^{-1} for xylenes, respectively, using all wind directions. While measured VOC mixing ratios agreed well with previous studies in Houston, showing clear diurnal variation due to boundary layer and emission source dynamics, the additional information collected from flux measurements not only showed the expected car-traffic source, but also strong evaporative emission sources during working hours that may not be accounted for. We estimated the potential amount of evaporative emission sources under the assumption that the simultaneously measured CO_2 emission was solely from vehicles in our footprint areas, and found that the proportion of evaporative emission was approximately 34% when integrated over the whole day. During winter, the mean and median fluxes were 0.38 mg m^{-2} h^{-1} and 0.31 mg m^{-2} h^{-1} for benzene, 0.43 mg m^{-2} h^{-1} and 0.32 mg m^{-2} h^{-1} for toluene, 0.06 mg m^{-2} h^{-1} and 0.05 mg m^{-2} h^{-1} for ethylbenzene, and 0.28 mg m^{-2} h^{-1} and 0.22 mg m^{-2} h^{-1} for xylenes, respectively. As these values were lower than during summer, particularly for toluene and xylenes, known to be used as solvents, temperature-driven evaporative emissions from onroad vehicles and solvent use at our location were obviously more prominent during the investigated summer period than averaged over the whole year.

The comparison of “top-down” results by our measured fluxes with “bottom-up” results by modeled ‘onroad’ and ‘nonpoint’ source categories in the EPA NEI suggested potential underestimates in the NEI by a factor of ~3 for benzene and ethylbenzene, and ~5 for toluene and xylenes. Higher offsets between the measured flux and the EPA NEI

occurred from the higher evaporative emission sources, which was more obvious in the comparison with the results in winter time.

Although the EPA estimates evaporative emissions from sources such as the light industrial metal-work and paint-shops surrounding our site, including the respective 'nonpoint' source category in our comparison did not lead to a match between upscaled measurements and the NEI. Hence, we conclude that a more sophisticated comparison is necessary to either verify that the NEI underestimates the amount or intensity of small scale area sources, such as solvent usage, or evaporative emissions from vehicles, or that the assumption of representativeness of our site is in error. Future work will therefore use the EPA traffic emissions models MOBILE6 and MOVES in conjunction with more detailed, seasonal traffic counts in this area. This and ongoing data acquisition and analysis can be used to validate and improve existing emission inventories, which in turn may improve numerical air quality modeling.

Mixing ratios and fluxes of biogenic VOCs including isoprene and its oxidation products MACR and MVK were also discussed. The presented results show that the mixing ratio and the flux of isoprene were affected by both anthropogenic and biogenic emission sources, as expected in this heterogeneous urban study area. During the morning rush hour, both the mixing ratio and the flux of isoprene showed peaks likely as a result of tail-pipe emissions, while during daytime biogenic emissions dominated. The observed mean and median daytime mixing ratio of isoprene was 0.40 ppb and 0.38 ppb,

respectively, and the flux of isoprene was 0.63 mg m^{-2} h^{-1} and 0.48 mg m^{-2} h^{-1} in the morning rush hour, and 0.46 mg m^{-2} h^{-1} 0.42 mg m^{-2} h^{-1} during daytime, respectively. A comparison of the diurnal variation of our measured flux with Guenther's model (Guenther et al. 1993) showed good agreement using a top-down calculated basal emission rate of 0.53 mg m^{-2} h^{-1}. The model results underestimated emissions during the morning rush hour, and for other daytime hours, partially affected by higher daytime isoprene loss due to photochemical removal and possibly also by anthropogenic emissions. We estimated that the anthropogenic isoprene source from tail-pipe emissions may have contributed up to 30% of the total amount of morning rush hour flux.

A semi-quantitative footprint analysis for surface emission source tracking was also carried out. The result showed two different patterns of surface contributions to fluxes: the daytime footprint was dominant over the southern part of our study domain with a relatively higher tree density, but the morning rush-hour was dominated by closer-by areas in the NE and SE, areas intersecting with the largest local, multi-lane commuter roads. This result also supported the notion of anthropogenic emissions of isoprene during morning rush hour.

Our investigation of isoprene's oxidation products MACR and MVK showed that both anthropogenic and biogenic emission sources exist for MACR, while MVK was clearly dominated by the biogenic source from isoprene oxidation. Anthropogenic sources for

MACR but not MVK become very clear in comparison to the isoprene data, both when comparing mixing ratios and fluxes. Our data indicate that both MACR and MVK at our site come from very recent additions. We hypothesized that both oxidation products are in fact formed from recent isoprene emissions in the footprint area, i.e. from isoprene being oxidized before it is sampled at our 60 m agl inlet. The concentration ratio of MVK to MACR at our site was close to the yield ratio from OH-isoprene chemistry, especially when an MACR background concentration from anthropogenic emissions (~ 40 ppt) was considered. Due to high ambient OH radical mixing ratios, we found that isoprene's lifetime is so short that 10-20% losses between emission and sampling points are feasible and would explain most if not all of the observed MVK flux. Instead, it would explain only roughly half of the measured MACR flux, the remaining half likely occurring as a result of tailpipe emissions.

Isoprene and MACR are not currently considered tailpipe emissions in emissions inventories. However, our results clearly show that both species are emitted in significant amounts by sources coincident with the morning rush hour period. Future work will compare our measured emissions to (i) various estimates from the most current emission data for tailpipe exhaust, and (ii) more detailed estimates of biogenic emissions from isoprene-emitting trees in the footprint area.

REFERENCES

Ackman, R.G., 1964. Fundamental groups in the response of flame ionization detectors to oxygenated aliphatic hydrocarbons. Journal of Gas Chromatography, 2(6), 173-179.

Ackman, R.G., 1968. Flame ionization detector - Further comments on molecular breakdown and fundamental group responses. Journal of Gas Chromatography, 6(10), 497-501.

Ammann, C. and Meixner, F.X., 2002. Stability dependence of the relaxed eddy accumulation coefficient for various scalar quantities. Journal of Geophysical Research-Atmospheres, 107(D8), 4071, doi: 10.1029/2001JD000649.

Andreas, E.L., Reginald, J.H., Gosz, J.R., Moore, D.I., Otto, W.D. and Sarma, A.D., 1998. Stability dependence of the eddy-accumulation coefficients for momentum and scalars. Boundary-Layer Meteorology, 86(3), 409-420.

Apel, E.C., Riemer, D.D., Hills, A., Baugh, W., Orlando, J., et al., 2002. Measurement and interpretation of isoprene fluxes and isoprene, methacrolein, and methyl vinyl ketone mixing ratios at the PROPHET site during the 1998 Intensive. Journal of Geophysical Research-Atmospheres, 107(D3), 10.1029/2000JD000225.

Atkinson, R., 1990. Gas-phase tropospheric chemistry of organic-compounds - A review. Atmospheric Environment Part A-General Topics, 24(1), 1-41.

Atkinson, R., 1994. Gas-phase tropospheric chemistry of organic-compounds. Journal of Physical and Chemical Reference Data Monograph(2), 1-216.

Baker, A.K., Beyersdort, A.J., Doezema, L.A., Katzenstein A., Meinardi, S., et al., 2008. Measurements of nonmethane hydrocarbons in 28 United States cities. Atmospheric Environment, 42(1), 170-182.

Baker, E.L., Smith, T.J. and Landrigan, P.J., 1985. The neurotoxicity of industrial solvents - A review of the literature. American Journal of Industrial Medicine, 8(3), 207-217.

Baker, J.M., Norman, J.M. and Bland, W.L., 1992. Field-scale application of flux measurement by conditional sampling. Agricultural and Forest Meteorology, 62(1-2), 31-52.

Baldocchi, D.D., Fuentes, J.D., Bowling, D.R., Turnipseed, A.A. and Monson, R.K., 1999. Scaling isoprene fluxes from leaves to canopies: Test cases over a boreal aspen and a mixed species temperate forest. Journal of Applied Meteorology, 38(7), 885-898.

Banta, R.M., Senff, C.J., Nielsen-Gammon, J., Darby, L.S., Ryerson, T.B., et al., 2005. A bad air day in Houston. Bulletin of the American Meteorological Society, 86(5), 657-669.

Berkowitz, C.M., Spicer, C.W. and Doskey, P.V., 2005. Hydrocarbon observations and ozone production rates in Western Houston during the Texas 2000 Air Quality Study. Atmospheric Environment, 39(19), 3383-3396.

Biesenthal, T.A. and Shepson, P.B., 1997. Observations of anthropogenic inputs of the isoprene oxidation products methyl vinyl ketone and methacrolein to the atmosphere. Geophysical Research Letters, 24(11), 1375-1378.

Biesenthal, T.A., Wu, Q., Shepson, P.B., Wiebe, H.A., Anlauf, K.G., et al., 1997. A study of relationships between isoprene, its oxidation products, and ozone, in the Lower Fraser Valley, BC. Atmospheric Environment, 31(14), 2049-2058.

Borbon, A., Fontaine, H., Veillerot, M., Locoge, N., Galloo, J.C., et al., 2001. An investigation into the traffic-related fraction of isoprene at an urban location. Atmospheric Environment, 35(22), 3749-3760.

Bowling, D.R., Turnipseed, A.A., Delany, A.C., Baldocchi, D.D. and Greenberg, J.P., et al., 1998. The use of relaxed eddy accumulation to measure biosphere-atmosphere exchange of isoprene and of her biological trace gases. Oecologia, 116(3), 306-315.

Businger, J.A. and Oncley, S.P., 1990. Flux measurement with conditional sampling. Journal of Atmospheric and Oceanic Technology, 7(2), 349-352.

Carter, W.P.L. and Atkinson, R., 1996. Development and evaluation of a detailed mechanism for the atmospheric reactions of isoprene and NO_x. International Journal of Chemical Kinetics, 28(7), 497-530.

Ciccioli, P., Brancaleoni, E., Frattoni, M., Marta, S., Brachetti, A., et al., 2003. Relaxed eddy accumulation, a new technique for measuring emission and deposition fluxes of volatile organic compounds by capillary gas chromatography and mass spectrometry. Journal of Chromatography A, 985(1-2), 283-296.

Dechapanya, W., Eusebi, A., Kimura, Y. and Allen, D.T., 2003. Secondary organic aerosol formation from aromatic precursors. 1. Mechanisms for individual hydrocarbons. Environmental Science & Technology, 37(16), 3662-3670.

Derwent, R.G., Middleton, D.R., Field, A., Goldstone, M.E., Lester, J.N., et al., 1995. Analysis and interpretation of air-quality data from an urban roadside location in Central London over the period from July 1991 to July 1992. Atmospheric Environment, 29(8), 923-946.

Desjardins, R.L., 1972. A study of carbon-dioxide and sensible heat fluxes using the eddy correlation technique. Ph.D. Dissertation, Cornell University, Ithaca, NY.

Dorsey, J.R., Nemitz, E., Gallagher, M.W., Fowler, D., Williams P.I., et al., 2002. Direct measurements and parameterisation of aerosol flux, concentration and emission velocity above a city. Atmospheric Environment, 36(5), 791-800.

Draper, T.H.J. and Bamiou, D.E., 2009. Auditory neuropathy in a patient exposed to xylene: Case report. Journal of Laryngology and Otology, 123(4), 462-465.

Dreyfus, G.B., Schade, G.W. and Goldstein, A.H., 2002. Observational constraints on the contribution of isoprene oxidation to ozone production on the western slope of the Sierra Nevada, California. Journal of Geophysical Research-Atmospheres, 107(D19), 4365, doi:10.1029/2001JD001490.

Fall, R. and Wildermuth, M.C., 1998. Isoprene synthase: From biochemical mechanism to emission algorithm. Journal of Geophysical Research-Atmospheres, 103(D19), 25599-25609.

Foken, T. and Wichura, B., 1996. Tools for quality assessment of surface-based flux measurements. Agricultural and Forest Meteorology, 78(1-2), 83-105.

Fortner, E.C., Zheng, J., Zhang, R., Knighton, W.B. and Molina L., 2009. Measurements of volatile organic compounds using proton transfer reaction - mass spectrometry during the MILAGRO 2006 Campaign. Atmospheric Chemistry and Physics, 9(2), 467-481.

Gallagher, M.W., Clayborough, R., Beswick, K.M., Hewitt, C.N., Owen, S., et al., 2000. Assessment of a relaxed eddy accumulation for measurements of fluxes of biogenic volatile organic compounds: Study over arable crops and a mature beech forest. Atmospheric Environment, 34(18), 2887-2899.

Gelencser, A., Siszler, K. and Hlavay, J., 1997. Toluene-benzene concentration ratio as a tool for characterizing the distance from vehicular emission sources. Environmental Science & Technology, 31(10), 2869-2872.

Gilman, J.B., Kuster, W.C., Goldan, P.D., Herndon, S.C., Zahniser, M.S., et al., 2009. Measurements of volatile organic compounds during the 2006 TexAQS/GoMACCS campaign: Industrial influences, regional characteristics, and diurnal dependencies of the OH reactivity. Journal of Geophysical Research-Atmospheres, 114, D00F06, doi:10.1029/2008JD011525.

Grabmer, W., Graus, M., Lindinger, C., Wisthaler, A., Rappengluck, B., et al., 2004. Disjunct eddy covariance measurements of monoterpene fluxes from a Norway spruce forest using PTR-MS. International Journal of Mass Spectrometry, 239(2-3), 111-115.

Grimmond, C.S.B., King, T.S., Cropley, F.D., Nowak, D.J., Souch, C., 2002. Local-scale fluxes of carbon dioxide in urban environments: Methodological challenges and results from Chicago. Environmental Pollution, 116, S243-S254.

Grosjean, D., Grosjean, E. and Gertler, A.W., 2001. On-road emissions of carbonyls from light-duty and heavy-duty vehicles. Environmental Science & Technology, 35(1), 45-53.

Guenther, A.B., Monson, R.K. and Fall, R., 1991. Isoprene and monoterpene emission rate variability - Observations with Eucalyptus and emission rate algorithm development. Journal of Geophysical Research-Atmospheres, 96(D6), 10799-10808.

Guenther, A.B., Zimmerman, P.R., Harley, P.C., Monson, R.K. and Fall, R., 1993. Isoprene and monoterpene emission rate variability - Model evaluations and sensitivity analyses. Journal of Geophysical Research-Atmospheres, 98(D7), 12609-12617.

Guenther, A., Hewitt, C.N., Erickson, D., Fall, R., Geron, C., et al., 1995. A global-model of natural volatile organic-compound emissions. Journal of Geophysical Research-Atmospheres, 100(D5), 8873-8892.

Guenther, A., Zimmerman, P., Klinger, L., Greenberg, J., Ennis, C., et al., 1996. Estimates of regional natural volatile organic compound fluxes from enclosure and ambient measurements. Journal of Geophysical Research-Atmospheres, 101(D1), 1345-1359.

Guenther, A., Geron, C., Pierce, T., Lamb, B., and Harley, P., et al., 2000. Natural emissions of non-methane volatile organic compounds, carbon monoxide, and oxides of nitrogen from North America. Atmospheric Environment, 34(12-14), 2205-2230.

Guenther, A., Karl, T., Harley, P., Wiedinmyer, C., Palmer, P.I., et al., 2006. Estimates of global terrestrial isoprene emissions using MEGAN (Model of Emissions of Gases and Aerosols from Nature). Atmospheric Chemistry and Physics, 6, 3181-3210.

Helmig, D., Greenberg, J., Guenther, A., Zimmerman, P. and Geron, C., 1998. Volatile organic compounds and isoprene oxidation products at a temperate deciduous forest site. Journal of Geophysical Research-Atmospheres, 103(D17), 22397-22414.

Henze, D.K., Seinfeld, J.H., Ng, N.L., Kroll, J.H., Fu, T.-M., et al., 2008. Global modeling of secondary organic aerosol formation from aromatic hydrocarbons: High- vs. low-yield pathways. Atmospheric Chemistry and Physics, 8(9), 2405-2420.

Jiang, G.F. and Fast, J.D., 2004. Modeling the effects of VOC and NOX emission sources on ozone formation in Houston during the TexAQS 2000 field campaign. Atmospheric Environment, 38(30), 5071-5085.

Jobson, B.T., Berkowitz, C.M., Kuster, W.C., Goldan, P.D., Williams, E.J., et al., 2004. Hydrocarbon source signatures in Houston, Texas: Influence of the

petrochemical industry. Journal of Geophysical Research-Atmospheres, 109, D24305, doi:10.1029/2004JD004887.

Jonsson, A., Persson, K.A. and Grigoriadis, V., 1985. Measurements of some low molecular-weight oxygenated, aromatic, and chlorinated hydrocarbons in ambient air and in vehicle emissions. Environment International, 11(2-4), 383-392.

Karl, T., Guenther, A., Jordan, A., Fall, R. and Lindinger, W., 2001. Eddy covariance measurement of biogenic oxygenated VOC emissions from hay harvesting. Atmospheric Environment, 35(3), 491-495.

Karl, T.G., Spirig, C., Prevost, P., Stroud, C., Rinne, J., et al., 2002. Virtual disjunct eddy covariance measurements of organic compound fluxes from a subalpine forest using proton transfer reaction mass spectrometry. Atmospheric Chemistry and Physics, 2, 279-291.

Karl, T., Jobson, T., Kuster, W.C., Williams, E., Stutz, J., et al., 2003. Use of proton-transfer-reaction mass spectrometry to characterize volatile organic compound sources at the La Porte super site during the Texas Air Quality Study 2000. Journal of Geophysical Research-Atmospheres, 108(D16), 4508, doi:10.1029/2002JD003333.

Karl, T., Apel, E., Hodzic, A., Riemer, D.D., Blake, D.R., et al., 2009. Emissions of volatile organic compounds inferred from airborne flux measurements over a megacity. Atmospheric Chemistry and Physics, 9(1), 271-285.

Katul, G.G., Finkelstein, P.L., Clarke, J.F. and Ellestad, T.G., 1996. An investigation of the conditional sampling method used to estimate fluxes of active, reactive, and passive scalars. Journal of Applied Meteorology, 35(10), 1835-1845.

Kean, A.J., Grosjean, E., Grosjean, D. and Harley, R.A., 2001. On-road measurement of carbonyls in California light-duty vehicle emissions. Environmental Science & Technology, 35(21), 4198-4204.

Kelly, J.L., Michelangeli, D.V., Makar, P.A., Hastie, D.R., Mozurkewich, M., et al., 2010. Aerosol speciation and mass prediction from toluene oxidation under high NO_x conditions. Atmospheric Environment, 44(3), 361-369.

Kljun, N., Rotach, M.W. and Schmid, H.P., 2002. A three-dimensional backward Lagrangian footprint model for a wide range of boundary-layer stratifications. Boundary-Layer Meteorology, 103(2), 205-226.

Kljun, N., Kastner-Klein, P., Fedorovich, E. and Rotach, M.W., 2004. Evaluation of Lagrangian footprint model using data from wind tunnel convective boundary layer. Agricultural and Forest Meteorology, 127(3-4), 189-201.

Kormann, R. and Meixner, F.X., 2001. An analytical footprint model for non-neutral stratification. Boundary-Layer Meteorology, 99(2), 207-224.

Kuster, W.C., Jobson, B.T., Karl, T., Riemer, D., Apel, E., et al., 2004. Intercomparison of volatile organic carbon measurement techniques and data at La Porte during the TexAQS2000 Air Quality Study. Environmental Science & Technology, 38(1), 221-228.

Kuzma, J. and Fall, R., 1993. Leaf isoprene emission rate is dependent on leaf development and the level of isoprene synthase. Plant Physiology, 101(2), 435-440.

Lamanna, M.S. and Goldstein, A.H., 1999. In situ measurements of C-2-C-10 volatile organic compounds above a Sierra Nevada ponderosa pine plantation. Journal of Geophysical Research-Atmospheres, 104(D17), 21247-21262.

Langford, B., Davison, B., Nemitz, E. and Hewitt, C.N., 2009. Mixing ratios and eddy covariance flux measurements of volatile organic compounds from an urban canopy (Manchester, UK). Atmospheric Chemistry and Physics, 9(6), 1971-1987.

Langford, B., Nemitz, E., House, E., Phillips, G.J., Famulari, D., et al., 2010. Fluxes and concentrations of volatile organic compounds above central London, U.K. Atmospheric Chemistry and Physics, 10(2), 627-645.

Martensson, E.M., Nilsson, E.D., Buzorius, G. and Johansson, C., 2006. Eddy covariance measurements and parameterisation of traffic related particle emissions in an urban environment. Atmospheric Chemistry and Physics, 6, 769-785.

McGaughey, G.R., Desai, N.R., Allen, D.T., Seila, R.L., Lonneman, W.A., et al., 2004. Analysis of motor vehicle emissions in a Houston tunnel during the Texas Air Quality Study 2000. Atmospheric Environment, 38(20), 3363-3372.

Mehlman, M.A., 1990. Dangerous properties of petroleum-refining products - Carcinogenicity of motor fuels (gasoline). Teratogenesis Carcinogenesis and Mutagenesis, 10(5), 399-408.

Milne, R., Mennim, A. and Hargreaves, K., 2001. The value of the beta coefficient in the relaxed eddy accumulation method in terms of fourth-order moments. Boundary-Layer Meteorology, 101(3), 359-373.

Monson, R.K., Jaeger, C.H., Adams, W.W., Driggers, E.M., Gary, M., et al., 1992. Relationships among isoprene emission rate, photosynthesis, and isoprene synthase activity as influenced by temperature. Plant Physiology, 98(3), 1175-1180.

Montzka, S.A., Trainer, M., Angevine, W.M. and Fehsenfeld, F.C., 1995. Measurements of 3-methyl furan, methyl vinyl ketone, and methacrolein at a rural forested site in the southeastern United States. Journal of Geophysical Research-Atmospheres, 100(D6), 11393-11401.

Montzka, S.A., Trainer, M., Goldan, P.D., Kuster, W.C. and Fehsenfeld, F.C., 1993. Isoprene and its oxidation products, methyl vinyl ketone and methacrolein, in the rural troposphere. Journal of Geophysical Research-Atmospheres, 98(D1), 1101-1111.

Myriokefalitakis, S., Vrekoussis, M., Tsigaridis, K., Wittrock, F., Richter, A., et al., 2008. The influence of natural and anthropogenic secondary sources on the glyoxal global distribution. Atmospheric Chemistry and Physics, 8(16), 4965-4981.

Na, K., Kim, Y.P. and Moon, K.C., 2003. Diurnal characteristics of volatile organic compounds in the Seoul atmosphere. Atmospheric Environment, 37(6), 733-742.

Nelson, P.F. and Quigley, S.M., 1983. The meta,para-xylenes-ethylbenzene ratio - A technique for estimating hydrocarbon age in ambient atmospheres. Atmospheric Environment, 17(3), 659-662.

Nemitz, E., Hargreaves, K.J., McDonald, A.G., Dorsey, J.R. and Fowler, D., 2002. Meteorological measurements of the urban heat budget and CO2 emissions on a city scale. Environmental Science & Technology, 36(14), 3139-3146.

Olaguer, E.P., Rappengluck, B., Lefer, B., Stutz, J., Dibb, J., et al., 2009. Deciphering the Role of Radical Precursors during the Second Texas Air Quality Study. Journal of the Air & Waste Management Association, 59(11), 1258-1277.

Olofsson, M., Ek-Olausson, B., Ljungstrom, E. and Langer, S., 2003. Flux of organic compounds from grass measured by relaxed eddy accumulation technique. Journal of Environmental Monitoring, 5(6), 963-970.

Pacifico, F., Harrison, S.P., Jones, C.D. and Sitch, S., 2009. Isoprene emissions and climate. Atmospheric Environment, 43(39), 6121-6135.

Pressley, S., Lamb, B., Westberg, H., Flaherty, J., Chen, J., et al., 2005. Long-term isoprene flux measurements above a northern hardwood forest. Journal of Geophysical Research-Atmospheres, 110, D07301, doi:10.1029/2004JD005523.

Qiao, F.X., Yu, L. and Vojtisek-Lom, M., 2005. On-road vehicle emission and activity data collection and evaluation in Houston, Texas. Energy and Environmental Concerns 2005(1941), 60-71.

Qin, Y., Walk, T., Gary, R., Yao, X. and Elles, S., 2007. C-2-C-10 nonmethane hydrocarbons measured in Dallas, USA - Seasonal trends and diurnal characteristics. Atmospheric Environment, 41(28), 6018-6032.

Rappengluck, B., Kourtidis, K., Melas, D. and Fabian, P., 1999. Observations of biogenic and anthropogenic NMHC in the greater Athens area during the PAUR campaign. Physics and Chemistry of the Earth Part B-Hydrology Oceans and Atmosphere, 24(6), 717-724.

Reimann, S., Calanca, P. and Hofer, P., 2000. The anthropogenic contribution to isoprene concentrations in a rural atmosphere. Atmospheric Environment, 34(1), 109-115.

Reiss, R., 2006. Temporal trends and weekend-weekday differences for benzene and 1,3-butadiene in Houston, Texas. Atmospheric Environment, 40(25), 4711-4724.

Rinne, H.J.I., Guenther, A.B., Warneke, C., de Gouw, J.A. and Luxembourg, S.L., 2001. Disjunct eddy covariance technique for trace gas flux measurements. Geophysical Research Letters, 28(16), 3139-3142.

Rinne, J., Douffet, T., Prigent, Y. and Durand, P., 2008. Field comparison of disjunct and conventional eddy covariance techniques for trace gas flux measurements. Environmental Pollution, 152(3), 630-635.

Roberts, J.M., Fehsenfeld, F.C., Liu, S.C., Bollinger, M.J., Hahn, C., et al., 1984. Measurements of aromatic hydrocarbon ratios and NO_x concentrations in the rural troposphere - Observation of air-mass photochemical aging and NO_x removal. Atmospheric Environment, 18(11), 2421-2432.

Roberts, J.M., Marchewka, M., Bertman, S.B., Goldan, P., Kuster, W., et al., 2006. Analysis of the isoprene chemistry observed during the New England Air Quality Study (NEAQS) 2002 intensive experiment. Journal of Geophysical Research-Atmospheres, 111, D23S12, doi:10.1029/2006JD007570.

Roth, M., 2000. Review of atmospheric turbulence over cities. Quarterly Journal of the Royal Meteorological Society, 126(564), 941-990.

Schade, G.W. and Goldstein, A.H., 2001. Fluxes of oxygenated volatile organic compounds from a ponderosa pine plantation. Journal of Geophysical Research-Atmospheres, 106(D3), 3111-3123.

Schnitzhofer, R., Beauchamp, J., Dunkl, J., Wisthaler, A., Weber, A., et al., 2008. Long-term measurements of CO, NO, NO_2, benzene, toluene and PM10 at a motorway location in an Austrian valley. Atmospheric Environment, 42(5), 1012-1024.

Singsaas, E.L. and Sharkey, T.D., 1998. The regulation of isoprene emission responses to rapid leaf temperature fluctuations. Plant Cell and Environment, 21(11), 1181-1188.

Singsaas, E.L. and Sharkey, T.D., 2000. The effects of high temperature on isoprene synthesis in oak leaves. Plant Cell and Environment, 23(7), 751-757.

Smith, L.A., Stock, T.H., Chung, K.C., Mukerjee, S., Liao, X.L., et al., 2007. Spatial analysis of volatile organic compounds from a community-based air toxics monitoring network in Deer Park, Texas, USA. Environmental Monitoring and Assessment, 128(1-3), 369-379.

Soegaard, H. and Moller-Jensen, L., 2003. Towards a spatial CO_2 budget of a metropolitan region based on textural image classification and flux measurements. Remote Sensing of Environment, 87(2-3), 283-294.

Song, Y., Shao, M., Liu, Y., Lu, S., Kuster, W., et al., 2007. Source apportionment of ambient volatile organic compounds in Beijing. Environmental Science & Technology, 41(12), 4348-4353.

Song, J, Vizuete, W., Kimura, Y. and Allen D.T., 2008. Comparisons of modeled and observed isoprene concentrations in southeast Texas. Atmospheric Environment, 42(8), 1922-1940.

Spaulding, R.S., Schade, G.W., Goldstein, A.H. and Charles, M.J., 2003. Characterization of secondary atmospheric photooxidation products: Evidence for biogenic and anthropogenic sources. Journal of Geophysical Research-Atmospheres, 108(D8), 4247, doi:10.1028/2002JD002478.

Starn, T.K., Shepson, P.B., Bertman, S.B., Riemer, D.D., Zika, R.G., et al., 1998. Nighttime isoprene chemistry at an urban-impacted forest site. Journal of Geophysical Research-Atmospheres, 103(D17), 22437-22447.

Stroud, C.A., Roberts, J.M., Goldan, P.D., Kuster, W.C., Murphy P.C., et al., 2001. Isoprene and its oxidation products, methacrolein and methylvinyl ketone, at an urban forested site during the 1999 Southern Oxidants Study. Journal of Geophysical Research-Atmospheres, 106(D8), 8035-8046.

Tambunan, P., Baba, S., Kuniyoshi, A., Iwasaki, H., Nakmura, T. et al., 2006. Isoprene emission from tropical trees in Okinawa Island, Japan. Chemosphere, 65(11), 2138-2144.

Trainer, M., Williams, E.J., Parrish, D.D., Buhr, M.P., Allwine, E.J., et al., 1987. Models and observations of the impact of natural hydrocarbons on rural ozone. Nature, 329(6141), 705-707.

Tuazon, E.C. and Atkinson, R., 1990. A product study of the gas-phase reaction of isoprene with the OH radical in the presence of NO_x. International Journal of Chemical Kinetics, 22(12), 1221-1236.

Valentini, R., Greco, S., Seufert, G., Bertin, N., Ciccioli, P., et al., 1997. Fluxes of biogenic VOC from Mediterranean vegetation by trap enrichment relaxed eddy accumulation. Atmospheric Environment, 31, 229-238.

Velasco, E., Lamb, B., Pressley, S., Allwine, E., Westberg, H., et al., 2005a. Flux measurements of volatile organic compounds from an urban landscape. Geophysical Research Letters, 32, L20802, doi:10.1028/2005GL023356.

Velasco, E., Pressley, S., Allwine, E., Westberg, H. and Lamb, B., 2005b. Measurements of CO_2 fluxes from the Mexico City urban landscape. Atmospheric Environment, 39(38), 7433-7446.

Velasco, E., Pressley, S., Grivicke, R., Allwine, E. and Coons, T., 2009. Eddy covariance flux measurements of pollutant gases in urban Mexico City. Atmospheric Chemistry and Physics, 9(19), 7325-7342.

Vlasenko, A., Slowik, J.G., Bottenheim, J.W., Brickell, P.C., Chang, R.Y.-W., et al., 2009. Measurements of VOCs by proton transfer reaction mass spectrometry at a rural Ontario site: Sources and correlation to aerosol composition. Journal of Geophysical Research-Atmospheres, 114, D21305, doi:10.1029/2009JD012025.

Warneke, C., Holzinger, R., Hansel, A., Jordan, A., Lindinger, W., et al., 2001. Isoprene and its oxidation products methyl vinyl ketone, methacrolein, and isoprene related peroxides measured online over the tropical rain forest of Surinam in March 1998. Journal of Atmospheric Chemistry, 38(2), 167-185.

Warneke, C., Luxembourg, S.L., de Gouw, J.A., Rinne, H.J.I., Guenther, A.B., et al., 2002. Disjunct eddy covariance measurements of oxygenated volatile organic compounds fluxes from an alfalfa field before and after cutting. Journal of Geophysical Research-Atmospheres, 107(D8), 4067, 10.1029/2001JD000594.

Whitworth, K.W., Symanski, E. and Coker, A.L., 2008. Childhood Lymphohematopoietic cancer incidence and hazardous air pollutants in Southeast Texas, 1995-2004. Environmental Health Perspectives, 116(11), 1576-1580.

Wiedinmyer, C., Friedfeld, S., Baugh, W. Greenberg, J., Guenther, A., et al., 2001. Measurement and analysis of atmospheric concentrations of isoprene and its reaction products in central Texas. Atmospheric Environment, 35(6), 1001-1013.

VITA

Name: Chang Hyoun Park

Address: Department of Atmospheric Sciences, Texas A&M University, 3150 TAMU, College Station, TX, 77843-3150

Email Address: jjamzang@ariel.met.tamu.edu

Education: B.S., Atmospheric Sciences, Pusan National University at Busan, Korea, February 1998
M.S., Atmospheric Sciences, Pusan National University at Busan, Korea, August 2000